IEEE Access
Multidisciplinary | Rapid Review | Open Access Journal

Date of publication xxxx xx, 2020, date of current version October 23, 2020.

Digital Object Identifier 10.1109/ACCESS.2017.DOI

Continuous Non-invasive Blood Pressure Monitoring: A Methodological Review on Measurement Techniques

TAI LE[1,*](STUDENT MEMBER, IEEE), FLORANNE ELLINGTON[1,*], TAO-YI LEE[2](STUDENT MEMBER, IEEE), KHUONG VO[2](STUDENT MEMBER, IEEE), MICHELLE KHINE[3], SANDEEP KRISHNAN[4], NIKIL DUTT[2,1](FELLOW, IEEE), AND HUNG CAO[1,3](SENIOR MEMBER, IEEE)

[1]Department of Electrical Engineering and Computer Science, University of California, Irvine, CA 92697, USA
[2]Department of Computer Sciences, University of California, Irvine, CA 92697, USA
[3]Department of Biomedical Engineering, University of California, Irvine, CA 92697, USA
[4]King's Daughters Medical Center, Ashland, KY 41101, USA
[*]These authors contributed equally to this work.

Corresponding authors: Nikil Dutt (e-mail: dutt@uci.edu) and Hung Cao (e-mail: hungcao@uci.edu).

This work was supported in part by the National Science Foundation under the CAREER #1917105 (H.C.)

ABSTRACT Continuous measurement of blood pressure is crucial to the assessment of many medical conditions. However, the current clinical gold standard involving an arterial catheter, occluding cuff, and other invasive procedures are performed in hospital settings while home-based devices can provide only intermittent measurement and are not as reliable. Therefore, there is a significant need for continuous non-invasive blood pressure (cNIBP) monitoring in the daily life. Pulse transit time (PTT)/pulse arrival time (PAT) - based blood pressure measurement has proven its potential to address this need. In this article, we present state-of-the-art devices and recent literature related to measurement technologies used in PTT/PAT - based methods for cNIBP monitoring. Various physiological signals which could be used to enable cNIBP in the home setting are categorized into two groups (i.e., proximal waveforms and distal waveforms) and are thoroughly discussed and compared. Given insightful analysis of these waveforms, we highlight their combinations to derive PTT/PAT values for BP measurement then discuss challenges presented from the cuffless and PTT/PAT - based nature of these devices. Finally, we conclude with future directions needed for home-based cNIBP adaptation and present societal broader impacts.

INDEX TERMS Continuous Non-Invasive Blood Pressure, Proximal waveform, Distal waveform, Pulse Transit Time, Pulse Arrival Time, Healthcare IoT.

I. INTRODUCTION

Continuous blood pressure monitoring in patient settings involves an invasive, oftentimes painful procedure that carries risks [1]. If done with an arterial line, it is painful to place and must stay affixed, increasing patient discomfort and possibility of infection. There is currently no good solution for continuous blood pressure monitoring in the outpatient setting which has been shown to be extremely beneficial to patient outcomes given blood pressure variability throughout the day. Recently, continuous non-invasive blood pressure (cNIBP) has become a viable option for patients needing long-term monitoring and preventive care, ideally in the home setting. The landscape of non-invasive blood pressure has been dominated by techniques reliant on Korotokoff sounds and oscillometry for more than 100 years [2]. Though these techniques were proven to be grounded on well-studied physiological phenomena, they lack the continuity that cNIBP could provide such as additional insights to prevent and understand diseases [3].

Blood pressure (BP), or pulse wave, is a *dynamic* physiological parameter that changes over time due to factors such as age, activity, and mental stress [4], [5]. Discrete BP measurements cannot fully reveal these dynamic characteristics of BP on individuals; hence, continuous BP monitoring can become much more informative if it is widely available and easy to obtain. Furthermore, cNIBP sensors can be feasibly designed to be cuffless and wearable. The Penaz method (volume clamp) and tonometry [2], [6] are popular cNIBP

methods. The Penaz method is cuff-based and optically measures the arterial volume in a limb, such as a finger or a toe, by applying pressure via an occluding cuff. The accuracy of volume clamp methods is known to be sensitive to the automatic recalibration process. Specifically, the volume clamp method often overestimates systolic BP [6]. Additionally, continual use of volume clamps increases the risk of venous congestion in the measuring site, and repeated and long-term wear to the same region become very uncomfortable and even painful for the subject, making this method not viable for long-term wear [6], [7]. Tonometry measures arterial pressure by applying force over a superficial artery to distort the vessel. This can be performed through a wristband or with a hand-held instrument and records pulsatility from applied force flattening the chosen superficial artery, which overcomes issues with blood vessel occlusion [2]. However, tonometry methods can become problematic as they are sensitive to imprecise placements of the device and easily result in inaccurate readings, especially with patient movement. Hence, establishing a calibrated baseline of tonometry readings remains challenging. The tonometry method may need to be paired with an occluding cuff to obtain calibrated results [3], [6].

Thus, to make cNIBP possible, alternative schemes are required. The use of pulse wave velocity (PWV) or its reciprocal, pulse transit time (PTT), is an attractive surrogate for cNIBP. In principle, PWV refers to the velocity at which pressure pulses propagate through the arterial tree. While traveling toward the peripheral arteries, the arrival times of a pressure pulse at two different sites (i.e., proximal and distal sites) of the arterial tree are detected, which results in PTT (Fig. 1.c). The PWV parameter was determined as the ratio between the distance between the two measurement sites (D) and PTT as shown in the follow equation.

$$PWV = \frac{D}{\text{PTT}} \tag{1}$$

The propagation of blood in the artery is very similar to that of the propagation of a compressible fluid. Indeed, the elasticity of an artery is related to the velocity of the volume pulses propagating through it, which can be described by the Moens-Kortweg (MK) equation [8]:

$$PWV = \sqrt{\frac{hE_0e^{\mathrm{a}P}}{\rho d}} \tag{2}$$

where h is the thickness in an elastic artery, d is the diameter, and ρ is the blood density. E_0 is the zero-pressure modulus in mmHg, and a is a constant that depends on the particular vessel (typically 0.016 mmHg^{-1} to 0.018 mmHg^{-1}). From (1) and (2), it indicates that high BP corresponds to high PWV, which in turn means a low PTT value. Given PTT/PAT-based method's potential for cNIBP, the following are commonly used steps for practical PTT/PAT-based cuffless BP monitoring [2], [9]:

1) Obtain proximal waveforms and distal waveforms.
2) Calculate PTT from the waveforms, either from foot-to-foot or peak-to-peak of the waveforms.
3) Calibrate various parameters to derive the relationship between PTT and BP.

Although PTT-based methods are promising, the wave propagation theory behind PTT via the MK and Hughes Equations is a subject of controversy. Experimental results showed that the elastic modulus E used in the MK equation depends not only on BP but also on the age of the central arteries [10], while BP and smooth muscle (SM) mainly affect the peripheral elasticity [11]. Therefore, reliance on the relationship between E and BP alone greatly impacts the accuracy of PTT/PAT-based BP estimation methods.

As described above, PTT has been proven as a powerful physiological parameter to derive BP with strong physiological mechanisms as evidenced by its involvement in the MK equation. Apart from PTT, pulse transit time (PAT) has captured great interest and thus been interchangeably used with PTT, which can create confusion between research questions, protocol development, and findings [12]. The discrepancy between these two is intuitively mentioned in a recent published book about cNIBP [2]. From the book, PTT is described as the time that an arterial pressure wave requires to propagate along the walls of a given segment of the arterial tree while PAT is the time at which an arterial pressure wave arrives at a certain point of the arterial tree. PAT can be measured as the time delay between the R-wave peak of the ECG signal and a particular point of the photoplethysmogram (PPG) signal, as shown in Fig. 6a. PAT is equal to the sum of PTT and the pre-ejection period (PEP) delay:

$$\text{PAT} = \text{PTT} + \text{PEP} \tag{3}$$

where PEP is the time needed to convert the electrical signal into a mechanical pumping force and isovolumetric contraction to open the aortic valve. PEP can be calculated by the delay between R-wave of ECG and impedance cardiogram (ICG) or the use of combination between phonocardiogram (PCG) and ICG signal [2], [6]. Due to its complexity when multiple physiological signals needed to get the PEP value, the use of PAT to estimate BP gains popularity. However, the accuracy of using PAT is still controversial [13]. Thus, another alternative approach requiring less physiological signals is proposed in [14]. The study shows that PEP accounts for 7% of the RR interval for approximately 20% of PTT measured at the fingertips at rest. In this review, we will cover measurement technologies using either PTT or PAT to estimate BP.

There have been numerous review papers summarizing various aspects of cNIBP (e.g., relationship among BP, PWV, and PTT/PAT; different BP models and algorithms to derive BP; and its feasibility for telemonitoring). Specifically, a theoretical exploration of PTT, PAT, and PWV to BP is rigorously investigated in [3], [15] while other review papers [16], [17] briefly mention about it. However, these works [16], [17]

are more focused on cNIBP's feasibility for telemonitoring, revealing challenges this technology needs to overcome in order to apply it to practical scenarios. Besides, cNIBP based on photoplethysmogram (PPG) has gained great interest as several papers [12], [18], [19] solely review this method. For instance, Wang and colleagues [18] intuitively provide PPG sensing principles of operation, PPG sensor circuit configurations for BP measurement, as well as different BP models and algorithms for calculating BP values. Single-site and multi-site PPG technologies are reviewed in [12], [19], which provides audience a broad overview on the use of PPG to derive BP. All those review papers show the theoretical exploration and potential approaches of cNIBP. Nevertheless, to the best of the authors' knowledge, there is a lack of a comprehensive review on various deployed physiological signals as well as measurement technologies for cNIBP.

In this context, our review aims to systematically elucidate procedures to enable reliably ubiquitous cNIBP monitoring via PTT/PAT. We first describe current state-of-the-art measurement technologies to obtain desired physiological signals (i.e., proximal and distal waveform) for cNIBP (Section II). Next, discussion on waveform combinations to achieve PTT/PAT value for BP estimation (Section III) as well as challenges of cNIBP for telemedicine are presented (Section IV). Finally, in the future direction (Section V), we provide some anticipation and recommendations for cNIBP monitoring in general and PTT/PAT-based methods in specific. It is worth noting that there is an increasing number of papers focusing on analyzing waveform morphology and using machine learning techniques to estimate BP from the derived features. Since this review paper is about instrumentation and PTT/PAT measurement techniques, such studies are not discussed in detail.

II. NONINVASIVE MEASUREMENT TECHNOLOGIES

Obtaining the proximal waveforms and the distal waveforms is the first step in PTT/PAT-based BP measurements. In this section, we first review measurement technologies to derive proximal waveforms and distal waveforms (Section II-A and B, respectively) and present the morphology and properties of those. The highlights of parts A and B are summarized in Tables 1 and 2, respectively.

A. MEASUREMENT TECHNOLOGIES TO ACQUIRE PROXIMAL WAVEFORMS

Proximal waveforms present cardiac electrophysiolgical information and are leading in time compared to distal waveforms due to the proximity of the sensor's placement to the heart. The following four signals are prominent proximal waveforms for BP technologies (Fig. 1d). Table I summarizes their signal morphologies, regions of interest, acquisition methods, advantages, and disadvantages.

1) Electrocardiogram

Electrocardiogram (ECG, or EKG) is a widely used biosignal in the medical field, especially in the clinical setting, for cardiovascular-related diagnosis and vital monitoring [20]. This waveform is also a common proximal waveform used in PTT/PAT-based BP derivation and is typically paired with photoplethysmogram (PPG) in cuff-less, non-invasive approaches using PAT or PTT [21]–[23]. This signal measures the small voltage changes in the electrical activity of the heart over time in each cardiac cycle by using electrodes attached on the body. In clinical settings, ECG electrodes are placed across the chest (precordium), lower arms, and lower legs with grounding electrodes to create a 12-lead ECG system, providing the clearest waveform [24]. This sensing technology is most commonly found in hospital and clinical settings while recently-developed approaches aim to be applicable for daily use in remote or home-based care [21]–[23]. Some of these home-based approaches include using 1-lead instead of 12-leads to record ECG and weaving the electrodes into textiles for signal acquisition [25], [26]. The waveform includes P waves, QRS complexes, and T waves, which provides more information about the heart than other waveforms such as PPG that usually displays one or two peaks. Current ECG methods for BP data acquisition include those employing machine learning or deep learning combined with PAT or PTT [27], [28].

2) Ballistocardiogram

The *Ballistocardiogram* (BCG) signal demonstrates the motion imparted to the body from the motion of the blood and the heart during each cardiac cycle. These repeated motions happen due to the rapid acceleration of blood when it is ejected and transferred into other vessels of the body during periods of relaxation and contraction, known as diastole and systole, respectively. In other words, BCG can provide information about the overall performance of the circulatory system, as it measures the mass movements, i.e., the mass of the circulating blood and the heart during the cardiac cycle [29]. The BCG waveform comprises several waves designated as H, I, J, K, and L. Although its morphological patterns are clearly defined, the understanding of this BCG wave is mainly based upon empirical correlations with other measurements such as ECG, phonocardiogram (PCG), and BP waveforms [30]. It is worth noting that BCG's morphology varies between subjects due to their postures, i.e., sleeping or sitting. Recent advances in electronics and sensing technologies have enabled sensors currently used for BCG signal data acquisition through various configurations and regions of interest (ROI), such as the wrist, ear, and feet on a scale-like platform or embedded in bed/chair [31]–[33]. For instance, a BCG-based sensor, namely muRata (*Nagaokakyo, Kyoto, Japan*), uses an ultra-sensitive accelerometer to capture the bed's vibrations generated by a subject's heart rate, respiration, and body movement. A microcontroller is used to process the information and provides heart rate, respiratory rate, heart rate variability, stroke volume measurements, and bed status indication [34]. Those sensors embedded in bed/chair are considered non-contact because they do not adhere to the body, which increases the

This article has been accepted for publication in a future issue of this journal, but has not been fully edited. Content may change prior to final publication. Citation information: DOI 10.1109/ACCESS.2020.3040257, IEEE Access

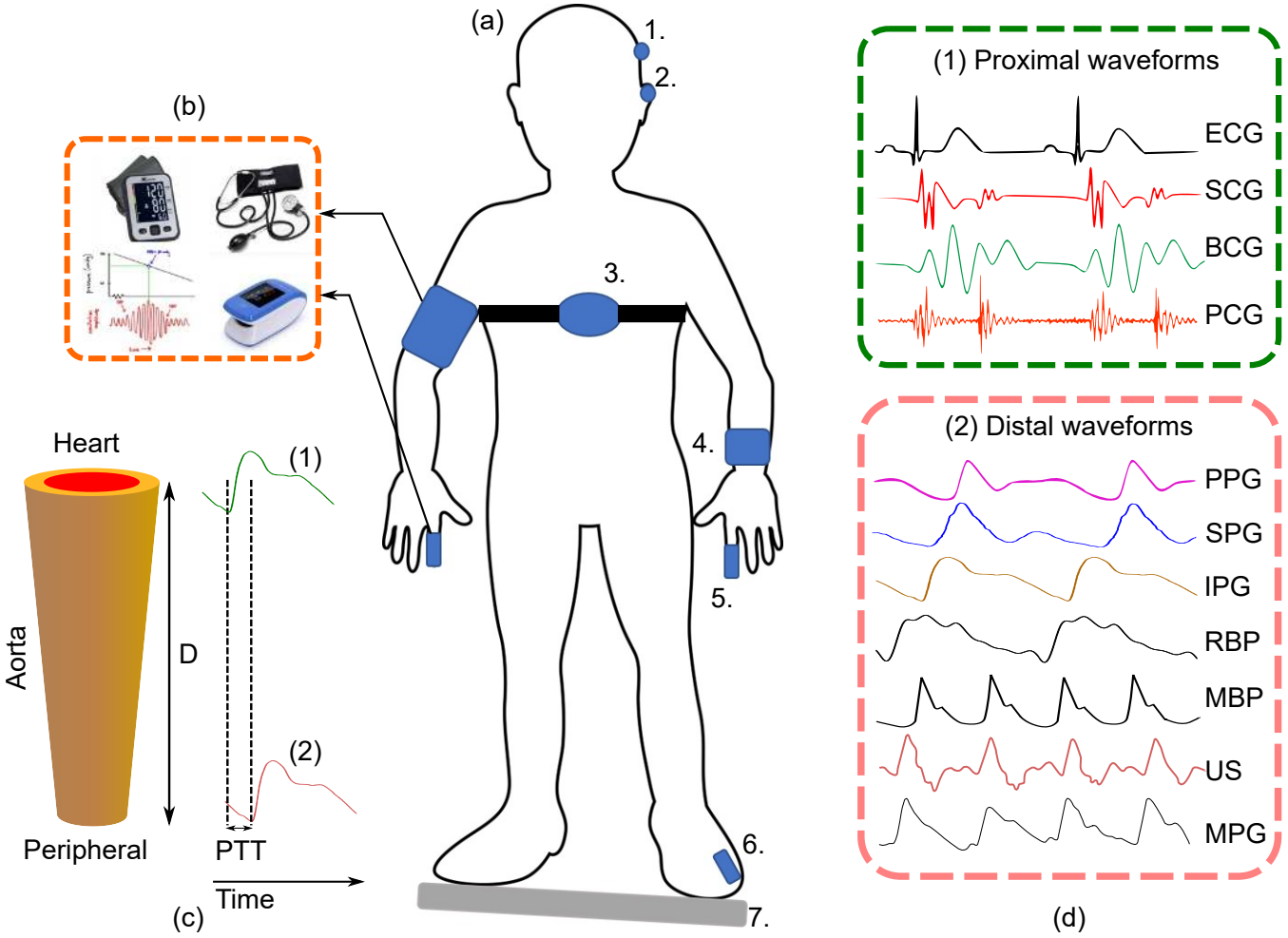

FIGURE 1: The overview of sensor's placement, proximal, and distal waveforms for cNIBP: (a) Common sensor's placement on body to acquire waveform for cNIBP (e.g., 1.-7.); (b) Commonly used calibration tools (cuff BP device, sphymomanometer, volume clamp); (c) Schematic diagram of the pressure pulse wave velocity propagate through the arterial tree; (d) Proximal and distal waveforms used to derive PTT value: proximal waveforms usually relates to cardiac-related activities signal, including electrocardiogram (ECG), Ballistocardiogram (BCG), Phonocardiogram (PCG) and Seismocardiogram (SCG). Distal waveforms usually used to measure pulse signal from artery peripheral, including photoplethysmogram (PPG), Speckleplethysmogram (SPG), impedance plethysmography (IPG), videoplethysmogram (VPG), Ultrasound (US), Magneticplethsmogram (MPG), radar-based pulse (RBP) and mechanical-based pulse (MBP).

applicability and users' comfort. Moreover, it can be used for a wide range of users (e.g., adults and children) in various care settings. However, it can be challenging due to the bed-based setup. If more people lay on the bed, it can induce extra motion, thereby causing errors in measurements. Another approach uses microelectromechanical (MEMS) gyroscopes to measure the angular Ballistocardiogram signal that is indicative of rotational movement of a subject's chest. The main advantage of these sensors is that it is not affected by gravity, which makes the measurement approximately independent of the position or posture of the monitored subject [35], [36]. Other types of sensors have also been investigated for BCG-based monitoring such as piezoelectric polyvinylidene fluoride (PVDF) sensors, electromechanical film (EMFi) sensors, pneumatic sensors, and fiber Bragg grating (FBG) sensors [37], [38]. While the use of PVDF sensors has proven to possess some advantages (e.g., user's comfort, a wide range of applications), EMFi sensors also have high sensitivity which is considered better than piezo materials. However, with high intrinsic resistance and bubble structures, the charge formed by a pressure applied to the sensor can be preserve for a long time. Besides, with high temperature (i.e., above 50 °C) applied, it may deteriorate the material.

3) Phonocardiogram

In additional to methods of diagnosing heart-related issues with the use of ECG or BCG, understanding the characteristics of the heart sound (HS), also known as heart auscultation, is another useful diagnostic method to get valuable infor-

mation of heart valves and heart hemodynamic functions. *Phonocardiogram* (PCG) is a diagnostic graphical method of recording sounds with the help of a specific equipment, namely phonocardiograph [39]. There are two dominant types of heart sounds, which are denoted respectively as S1 and S2, corresponding to the beginning of the ventricular systole and the onset of the ventricular diastole [40]. Auscultation with a stethoscope provides clinical information (e.g., the timing, relative intensity, frequency, quality, tone, and timbre) that can help in the diagnosis of the patient. PCG is usually collected by an acoustic device (i.e., stethoscope) attached at the surface of the chest wall, and it is used to register heart sounds and murmurs in the diagnosis of heart disease. With recent advancement in electronic technologies, the digital stethoscope has been significantly assisting physicians in managing and providing patient care [41].

4) Seismocardiogram

Seismocardiogram (SCG) is another non-invasive technique that measures cardiac-induced mechanical vibrations on the chest surface, including frequencies below the human hearing threshold. It is characterized by several peaks and valleys, and some of these displacements are associated with the opening and closure of the aortic valve (AO and AC) and the opening and closure of the mitral valve (MO and MC) [42]. There are many different methods used for SCG measurement; however, the use of lightweight low-noise accelerometers is most preferable as these sensors can be embedded inside portable or even wearable systems. This allows unobtrusive long-term monitoring of body accelerations in a wide range of conditions. Sensors are most commonly placed on the sternum or on its left lower border. However, other ROIs around the chest are used for SCG signal acquisition. SCG measurement methods and their placements are detailed in a review paper recently published [43].

B. MEASUREMENT TECHNOLOGIES TO ACQUIRE DISTAL WAVEFORM

In PTT/PAT-based BP measurements, the distal waveform is lagging in comparison to the proximal waveform, representing a phase delay between these two. The phase delay presents the change of blood volume that propagates from two different sites. The fingers and wrists are the most dominant positions to collect distal waveforms. In this section, we review measurement technologies to obtain the distal waveform (Fig. 1d). Table II summarizes the following signals, their regions of interest, acquisition methods, advantages, and disadvantages.

1) Photoplethysmogram

Photoplethysmogram (PPG) is an optical measurement commonly used in pulse oximetry in clinical settings for obtaining oxygen saturation information. This optical technique measures the amount of blood flowing in a region of interest (ROI) through the amount of optical absorption or reflection in the optical path. In other words, the PPG detects the change

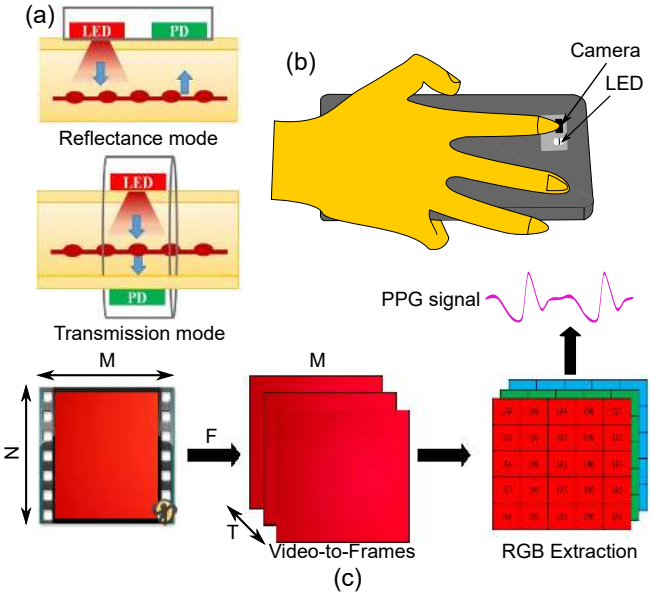

FIGURE 2: Methodology of PPG waveform acquisition: (a) Two different modes with the use of PPG sensor adapted from [46]: Reflection mode and Transmission mode; (b) A collected PPG signal with the smartphone through the camera and LED; (c) Procedures to extract the PPG signal through video collected by a smartphone.

of blood volume through a photoelectric technique [47]. PPG sensors can be classified into two separate measurement configurations: transmission mode and reflection mode (Fig. 2a). In the transmission mode, the sensor setup includes a light emitted diode (LED) on one side of the tissue serving as the ROI and a photodetector (PD) on the opposite side of the tissue. In this configuration, the emitted light is transmitted through the tissue and modulated by the underlying vasculature; the modulated optical energy is then detected at the other side. In the reflection mode, the two components (i.e., LED and PD) are on the same side of the tissue, usually on the same plane. The optical signal penetrates into the tissue, and the PD will receive the reflected light back with some fluctuations due to the tissue's absorption. While the transmission mode is mainly limited to the earlobe, fingertip, and toe, the reflection mode is applicable to additional locations as long as the ROI is a flat area (e.g. the forehead, forearm, supraorbital artery, under the legs, and the wrist) [9].

As mobile device technologies are rapidly being developed and improved upon, the typical features set in a smartphone today include high resolution cameras, high-end processors, built-in sensors such as accelerometer, orientation sensor, light-sensor, microphone, and light-emitting diode flashes (LEDs). Thus, instead of using it just as a device for storing and visualizing measured data, smartphones could be a suitable platform in several areas related to patient health due to its mobility, connectivity, and processing capabilities. Several studies [48]–[50] have been using smartphone as a source of collecting the PPG signal. It takes advantage of camera and

This article has been accepted for publication in a future issue of this journal, but has not been fully edited. Content may change prior to final publication. Citation information: DOI 10.1109/ACCESS.2020.3040257, IEEE Access

TABLE 1: Proximal waveforms for BP Measurement

Signal	Description	ROIs	Acquisition Methods	Advantages	Disadvantages
Electrocardiogram (ECG) [20]–[24]	a graph of voltage versus time of the electrical activity of the heart	chest, lower arms, and lower legs; contact/non-contact method to acquire ECG [24]	PTT/PAT (acts as a proximal signal, combined with other signals) [20], [22], [23]	high reliability of the R-wave detection, robustness to motion artifacts, wearable applications [9], [44]	inconvenient to setup, induce PEP which results errors in BP estimation [2], [44]
Ballistocardiogram (BCG) [29], [30]	the recording of motion imparted to the body by the motion of blood and the heart during each cardiac cycle	wrist, ear, feet on scale-like platform and embedded in bed/chair [31]–[33]	PTT (acts as a proximal signal, combined with ECG and PPG; J-K amplitude-based BP estimation	Easy to set up, signal can be acquired in various body's locations,	BCE's morphology significantly changes based on sensor's location, susceptible to motion artifact [35], [37]
Seismocardiogram (SCG) [42], [43]	a non-invasive technique that measures cardiac-induced mechanical vibrations at the chest surface including those below the human hearing threshold	the sternum, its left lower border, or the chest wall [42], [43]	PTT (from AO of SCG to peak of PPG); RAC interval (AVC point of SCG to the R peak of ECG	inexpensive and unobtrusive, the signal can be accurately measured by phone's built-in accelerometer [45]	require precise location of sensor and the axes orientation to get high quality signal; sensitive to motion artifact
Phonocardiogram (PCG) [39]–[41]	diagnostic graphical method of recording sounds, echoes that accompany mechanical vibrations originating in the heart and vessels	a stethoscope placed in the surface of chest wall	PTT/VTT (time interval between S1 of PCG and the peak of PPG)	Inexpensive, easy to set up	low amplitude, susceptible to motion artifact

Abbreviations: ROIs = region of interests, PEP = Pre-ejection period, AO = The aortic valve opening in the SCG signal, PTT = pulse transit time, VTT = vascular transit time, PAT = Pulse arrival time, AVC = The aortic valve closing in the SCG signal, PCG = Phonocardiogram, BCG = Ballistocardiograph, PPG = Photoplethysmogram, SCG = Seismocardiogram.

built-in LEDs from the smartphone. Subjects cover a smartphone camera lens with their fingertip, try to hold their finger steady, and press without additional force as shown in Fig. 2b. The raw video with the size of $N \times M$ pixel is collected and then extracted into different T frames containing different channels (i.e., red, blue, and green channel) as described in Fig. 2c. Thus, the PPG signal subsequently is calculated by taking the average brightness of either red or green channel in each frame [50], [51].

Since the volume and distension of the arteries can be related to the pressure in the arteries, the PPG signal produces pulse waveforms that are morphologically similar to pressure waveforms [9]. Therefore, many studies have been investigating alternative methods to estimate BP through either only PPG signal or the combination of PPG signal and other physiological signals such as ECG, BCG, PCG, and IPG, which are comprehensively reviewed in Section III.

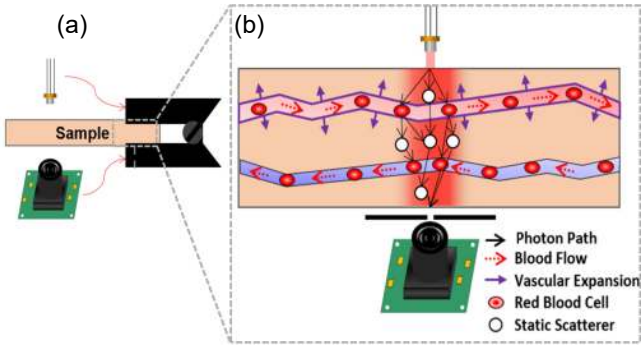

FIGURE 3: Hardware component description: (a) Hardware configuration of the SPG/PPG Finger-Clip; (b) Physiological view of vessel during SPG and PPG measuring; adapted from [52].

2) Speckleplethysmogram

Speckleplethysmogram (SPG) has been recently used as an alternative to PPG for measuring heart rate variability (HRV) [52], [53]. SPG is an optical method based on laser speckle contrast imaging (LSCI) to monitor changes in blood flow [54]. This technique is also referred to as Affixed Transmission Speckle Analysis (ATSA) [52]. SPG devices utilize a laser source that emits a scatter of small rays through the thickness of the tissue into a CMOS camera on the other side, depicted in Fig. 3a. The camera records a raw video with at least 30 frames per second (fps) and runs image processing techniques to identify the speckles from the laser in the red channel of each frame. To measure, the user places a finger tip in the clip-on, which further improves signal quality by reducing motion artifacts. The amount of speckles detected in the image correlates to the volume of blood present at that time point, and the change over time forms the SPG waveform. Studies comparing the signal to PPG report a higher signal to ratio (SNR) to the latter in situations with more motion and colder climates [52], [53]. In terms of light exposure, SPG has not been compared to PPG in this aspect, but SPG tests are currently conducted in dark rooms. Similar to PPG, SPG could be measured through smartphones as there are methods using LSCI for skin blood flow acquisition [54], [55]. Although smartphones and low-

grade cameras, even with the newest models, cannot capture raw images at a fast enough rate to create a video with 30 fps, the algorithms in [54], [55] can be used on standard mp4 videos to derive SPG by adjusting the camera's parameters to have the speckles recorded shown larger than a pixel.

3) Mechanical-based pulse measurements

The arterial pulse is an important vital sign, containing a wealth of cardiovascular information such as systolic BP (SBP) and diastolic BP (DBP). The pulse is produced as a result of the sudden ejection of blood into the aorta and its transmission throughout the arterial system [56], and it is expanded in response to the blood volume change through vessel (Fig. 4b). The arterial pulse rate can be palpated in any of the body's accessible sites, including the carotid artery, brachial artery, and radial artery (Fig. 4a). To monitor the epidermal pulse waves, several non-invasive methods have been studied. From the remarkable advances in technology, mechanical-based pulse measurement (e.g., capacitive, ferroelectric, or piezoresistive sensors) have been made into non-invasive health-monitoring devices with ultraconformal and stretchable capabilities [57]–[59].

For BP monitoring, although tonometry suffers of some limitations, this method inspired several research groups to develop alternatives in the arterial pulse detection, creating tonometry-based BP measurements that are more conformable to the body. Meng et al. [60] demonstrated a weaving constructed of self-powered pressure sensors (WCSPS) for continuous monitoring of pulse wave velocity (PWV) and BP. The system achieved a sensitivity of 45.7 mV Pa^{-1}, and no performance degradation was observed after 40,000 cycles of continuous operation. Fig. 4c shows the WCSPS were directly worn at the fingertip and wrist. The authors simultaneously measured the pulse waves from the subject's fingertip and ear, thereby identifying the PTT interval as the time difference between two pulse waves. The study was tested on 100 participants with different health statuses and showed minimum discrepancy between SBP and DBP measured by the WCSPS versus a cuff-based BP device (1.41 % and 0.87% respectively). Luo et al. [61] proposed a flexible piezoresistive sensor (FPS) patch and epidermal ECG sensors for cuff-less BP measurement with PTT as shown in Fig. 4d. The time interval between the R peaks of the ECG signal and the maximum points of the arterial pulse were calculated and correlated with BP simultaneously recorded by a BP standard device. The FPS was developed with the integration of multiple materials, including a PI substrate, a pair of interdigitated Au electrodes, carbon-decorated fabric, and PEN encapsulation, letting the sensor maintain mechanical flexibility. The DBP of the FPS/ECG-based method showed $<$ 4 mmHg mean absolute difference compared with the benchmark. Dagdeviren et al. [62] proposed a piezoelectric sensor developed on an elastomer substrate with ultrathin inorganic piezoelectric and semiconductor materials. To determine PWV for BP measurement, three configuration cases were tested. Two sensors were placed on: 1) the carotid artery of neck and lateral epicondyle vessel of the arm; 2) the lateral epicondyle vessel and radial artery of the wrist; and 3) near epicondyle vessel and radial artery (Fig. 4e). The PWV values from setups 1, 2, and 3 were $\sim$5.4 ms^{-1}, $\sim$5.8 ms^{-1} and $\sim$6.5 ms^{-1} respectively. Thus, these results were comparable with the typical aortic PWV ($\sim$4.5 ms^{-1}) measured by tonometry. In addition to these sensors, fiber Bragg grating (FBG) sensors have been used for mechanical-based pulse measurement. Haseda et al. [38] presented an FBG sensor fabricated in plastic optical fibers to obtain pulse wave signals at brachial artery locations. The authors recorded the pulse wave signal and reference BP simultaneously in four subjects with 120 recordings in total, then partial least squares regression was deployed to estimate BP. However, due to a small number of participants, the accuracy of BP estimated via FBG sensory signals was not high (e.g., the correlation coefficients of SBP and DBP are less than 0.80).

4) Impedance Plethysmogram

Impedance plethysmogram (IPG) is an electrical impedance-based, non-invasive medical diagnostic signal which records small changes in the blood volume in terms of the electrical bioimpedance of a body part (e.g., chest, limb, and calf). The impedance measured in IPG provides information about the tissue property of the body, and hence it can be used to indirectly study and analyze the tissue health and functionality of a human subject [63]. To collect the IPG signal, a tetrapolar configuration is usually deployed as shown in Fig. 5a. Specifically, four conductive electrodes are place around the body part or limb. An AC current with low amplitude (5 mA) and low frequency (50 kHz – 100 kHz) is passed through the two outer electrodes, and the change in electrical impedance is measured across the inner electrodes. While this method holds potential for BP diagnosis, the most significant challenge for the IPG technique is the optimal placement of the electrode array because the current distribution will be affected by body tissue and muscle [64]. Moreover, the signal is susceptible to motion artifacts [65] and attenuated due to the skin electrode impedance error [63]. In IPG theory, a shunting impedance (Z_b), including the impedance of artery (Z_a) and tissue (Z_t) in parallel, is produced as shown in the following equation for each pressure pulse induced by the blood flow through the limb.

$$Z_b = \rho_b \frac{L}{\Delta A} \tag{4}$$

where ΔA is the area of the artery that increases when an extra amount blood goes to the limb. L is the length of the segment being measured. ρ_b is blood resistivity. Given this equation and combining it with the PTT-based BP measurement approach, Huynh et al. [44] proved IPG's relation to BP, and the IPG obtained has been used to measure a proximal waveform for PTT estimation through the central arteries. This relationship is depicted in the following equation:

This article has been accepted for publication in a future issue of this journal, but has not been fully edited. Content may change prior to final publication. Citation information: DOI 10.1109/ACCESS.2020.3040257, IEEE Access

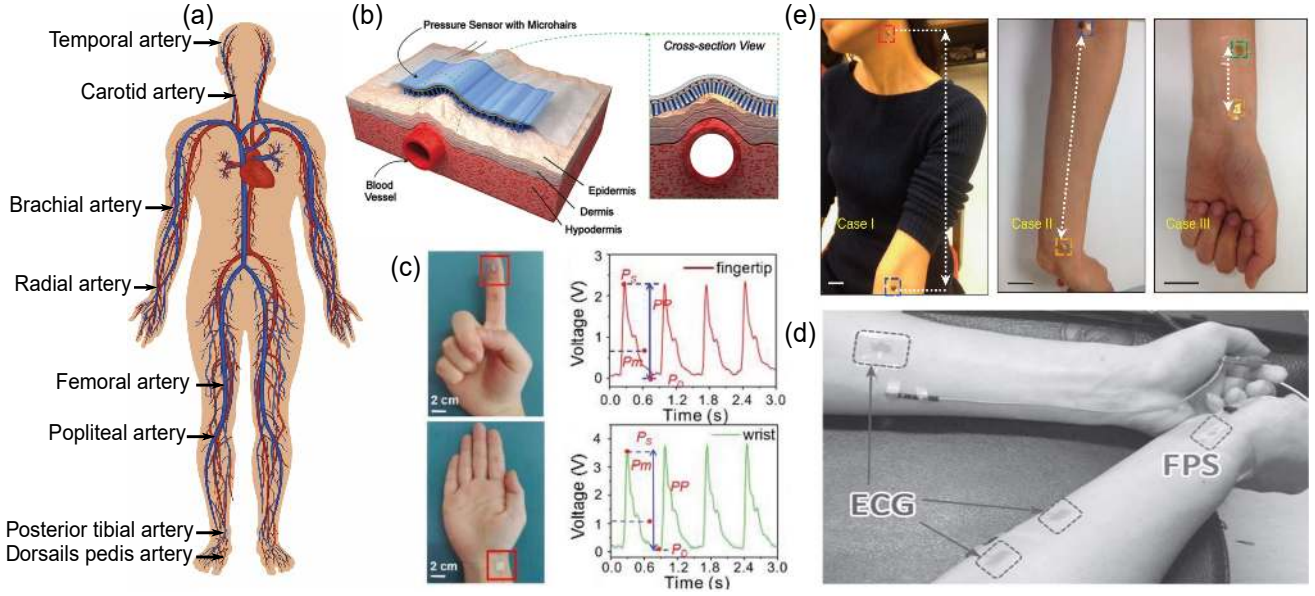

FIGURE 4: Mechanical-based pulse measurement overview and recent studies: (a) Accessible arterial pulse sites; (b) Schematic illustration to detect pulse on a human's neck with a microhair sensor. Adopted from [57]; (c) Representative pulse waveforms and locations for measurement with the WCSPS. Adopted from [60]; (d) The sensor patch containing FPS and epidermal ECG sensors for BP measurement. Adopted from [61]; (e) Illustration of PWV parameter determination with two pair piezoelectric sensors. Adopted from [62].

$$P(t) = P_0 + \rho \frac{D^2}{\text{PTT}^2} \ln\left[1 + K(Z_0 - Z(t))\right] \qquad (5)$$

K is a constant and is equal to Z_{a0}/Z_0^2. At the pressure P_0, Z_{a0} represents the arterial impedance. Z_0 is the impedance of the body segment while $P(t)$ can be replaced by SBP or DBP.

5) Radar-based pulse measurement

Radar in the medical setting can be used to measure arterial pulse waves, ventricular motion, and pulse-pressure, which are parameters correlated with blood pressure [67]–[70]. Pulse waves are generated by the radar machine and pass through the aortic artery, generating vasomotion. This movement is detected on the surface of the body by the device through two methods: with or without any contact antennas on the subject. Random body motion is considered and filtered out through Doppler radar methods [67]. Low noise amplifiers are applied to increase readings of cardiac-related motion. Applications of this system include antennas on the user's sternum, non-contact units from a distance, and a wearable wrist device [67]–[70]. Currently, the signal is robust in stationary positions before and after exercise for non-contact and wearable devices and has potential for long-term CNIBP monitoring for remote healthcare. However, safety is a concern for radar systems as the device emits continuous waveforms propagating into the subject body; thus, the range of frequency should be closely monitored to allow continuous measurements without injury [67]–[70].

6) Video Plethysmogram

Video Plethysmogram (VPG) is a proven method for BP acquisition in contactless and non-invasive measurements using video analysis as the medium [71], [72]. This technique has potential to be used in remote health monitoring in hospitals, elderly homes, workplaces, and with drivers to detect anomalies in health conditions [72]. Similar to PPG, VPG monitors BP from the reaction of light on the ROI. Light emitted on the tissue is absorbed and then partially reflected on the surface with the amount of absorbed light varying depending on the hemoglobin present in the bloodstream at that time [71]. The peak of light absorption corresponds to a reflected green light being captured by the video camera, which is positioned at a fixed distance facing the ROIs (Fig. 1). Thus, recording and analyzing the green channel of the video frames reflect the change of blood present [72]. This method is prone to noise when the user is in motion or the camera used does not meet the proper requirements. Thus, when measuring, the patient is sitting in a fixed position in front of the camera. For better readings, using the forehead as the ROI provides higher SNR than the palm in PTT-based methods. Elevation of the ROI compared to the heart is also considered in VPG BP measurements [73].

7) Magnetic Plethysmography

Magnetic plethysmography (MPG) detects fluctuations caused by blood flow in an emitted ambient magnetic field encompassing the monitored blood vessel for PWV measurements. This is achieved through using MPG transducers in an arterial-compliance probe to create a local PWV reading

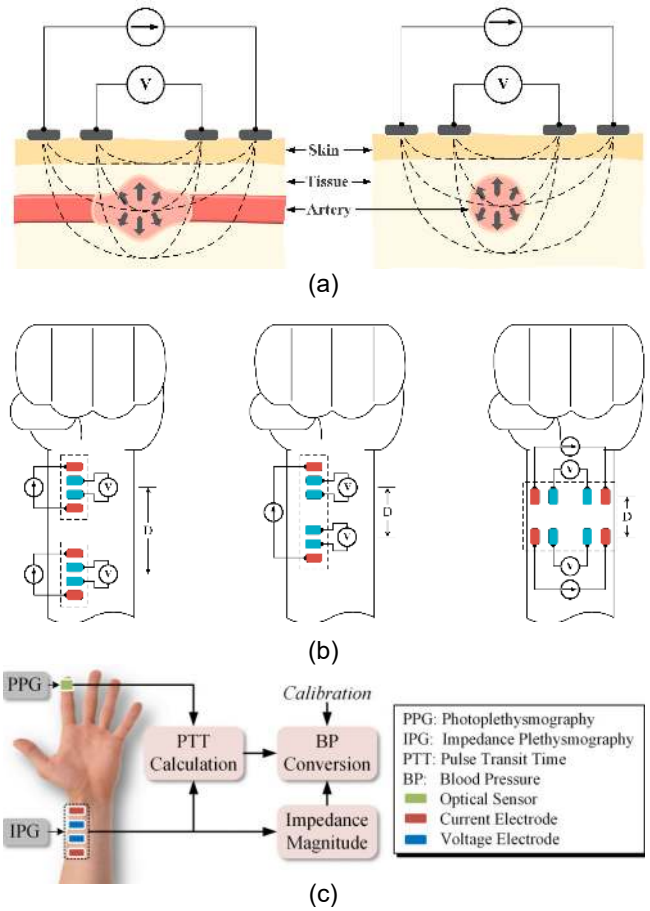

FIGURE 5: The genesis of IPG measurement and its configuration: (a) Tetrapolar configuration of electrodes.; (b) Distribution of two pair IPG signals with different distance for PWV measurement. Adopted from [66]; (c) Block diagram of the proposed PTT-IPG-based BP model with the use of IPG signal and PPG signal. Adopted from [44].

[74]–[76]. MPG is another potential approach to clinical non-invasive BP acquisition and is a comparable and less expensive BP method to ultrasound. The device is composed of at least one magnet, either an electromagnet or a permanent magnet, with an excitation coil and potentially a compensation coil that helps facilitate control over the magnetic field generated. This is for ensuring an easy magnetic biasing near the sensor while producing a strong enough field to encompass the artery beneath the skin. An electromagnet is more flexible in design than a permanent magnet, which is ideal for making compact devices without undermining the output quality from the relative geometry of the system being changed [74]. MPG has been demonstrated to be used in carotid and radial probes and finger cuff PWV approaches for BP measurement. To create a PWV reading using MPG, two single probes or one single dual probe is used. For the single probes, one was placed on the carotid artery and the other on the radial artery separate locations while the dual probe can measure PWV within a small distance (23 mm distance apart) [74], [76].

8) Ultrasound-based pulse measurement

Ultrasound (US) is a clinical approach to monitor BP in a non-invasive and non-occlusive manner. This technique can not only monitor blood velocity and blood volume flow but also report the probed vessel's wall thickness and diameter waveforms (Fig. 4b) [77]–[79]. In non-invasive cuff-less approaches, a US probe is held against the carotid artery and continuously measures while in contact (Fig. 6a). The carotid artery is chosen due to the ROI possessing a strong central DBP and SBP compared to more commonly used brachial measuring in clinical practice as well as many models and equations existing to detail the tissue of the throat [79]. PWV is used in US methods opposed to PTT as the accuracy of PTT can be prone to error from incorrect measurement and difficulty with small transit timer, especially in the ROI [80]. The method of deriving cuff-less carotid BP from this signal varies depending on the angle, pressure, calibration, and pairing with other sensors. US based BP acquisition demonstrates a good SNR in stationary positions.

III. PTT/PAT-BASED BP METHOD: STATE OF THE ART

With a variety of proximal and distal waveforms described in Section II, we review recent state-of-the-art approaches reported in literature that deploy different combinations between proximal and distal waveforms to enable PTT/PAT-based BP monitoring. It is categorized based on the proximal waveform used. In this section, we also summarize studies using single waveform acting as a distal and proximal waveform to derive the PTT value for cNIBP. Table 3 reports key details of the experiments reported in Section III.

1) Using ECG as a proximal waveform

As an ECG signal has distinct peaks (PQRST) in its waveform and is simple and inexpensive to obtain, it is usually used as a proximal waveform for BP acquisition, being paired with PPG, SPG, radar, and VPG. PAT is defined as the delay between the QRS peaks in ECG and the corresponding points in PPG. Cattivelli et al. [21] uses the MIMIC database to test their algorithm based on PAT to improve auto-calibration and robustness of ECG-PPG based SBP and DBP estimation. The configuration reported SBP within a standard deviation of 7.77 mmHg and DBP within 4.96 mmHg and needed re-calibration each hour [21].

Alongside PAT methods, PTT can be used to estimate arterial BP by measuring the time interval between the R-wave of an ECG waveform and the corresponding point in a PPG signal as shown in Fig. 6a [22], [23]. Shriram et al. [22] used PTT in their ECG-PPG configuration to estimate SBP. With attached electrodes and LED/photo detector sensors on a subject, the BP compared to the reference sphygmomanometer had a mean and standard deviation of -0.34±3.1 mmHg [22]. This method demonstrates PTT from ECG and PPG as an easier method of measuring for the comfort of patients and portability for continuous, long term monitoring;

TABLE 2: Distal Signals for BP Measurement

Signal	Description	ROIs	Acquisition Methods	Advantages	Disadvantages
Photo plethysmography (PPG) [9], [46]–[51], [81]–[84]	an optical technique that measures the change of blood volume by photoelectric technique as well as measures the oxygen saturation in the blood	**Transmission Mode:** earlobe, fingertip, toe **Reflectance Mode:** forehead, forearm, supraorbital artery, under the legs, and the wrist [46]	slope transit time [81], arterial PTT [82], blocking-free optical-oscillometry [83], arteriolar PTT [84]	inexpensive, simple set up	external light and cold temperatures can add noise to data
Speckle plethysmography (SPG) [52]–[55]	an optical technique using laser speckle contrast imaging (LSCI) to monitor changes in blood flow	finger [52], [53], wrist [54], [55]	Laser Speckle Contrast Imaging [52]–[55]	higher SNR compared to PPG in situations with more motion and cold climates, wearable sensors [52], [53]	External Light can affect data and add noise [52], [53]
Mechanical-based [56]–[62]	measuring the ejection of blood into the aorta and its transmission throughout the arterial system and it is expanded in response to the blood volume change through vessel; mechanical-based BP measurements include capacitive, ferroelectric, or piezoresistivesensors	carotid artery, brachial artery, radial artery	PTT [61], [62] and PWV [60]	ultraconformal and stretchable capabilities	Precise placement of measuring technolgy is needed for accurate results
Impedance Plethysmography (IPG) [44], [63]–[66], [85]	an electrical impedance based noninvasive medical diagnostic procedure which measures small changes in the blood volume in terms of its electrical bioimpedance of a body part	finger [44], [85], wrist [66]	PTT (with Proximal or Distal Signals) [44], [66], [85]	cuff-less approach to BP acquisition	current affected by body tissue/muscle [64]; susceptible to motion artifacts [65]; skin electrode impedance error [63]
Radar [67]–[70]	generated pulse waves that pass though the aortic artery, creating vasomotion that measure arterial pulse waves, ventricularmotion, and pulse-pressure, which are correlated to blood pressure	sternum (aortic artery) [67]–[69], wrist [70]	PAT and PTT with bioimpedence and ECG [67], pulse pressure from stroke volume [68], carotid-femoral PTT [69]	non-contact or wearable options [68]–[70]; before or after exercise long term acquisition; no individual calibration	distance of device and user's position is limited for more accurate measurement, bulky, stationary [68], [69]
Video Plethysmography (VPG) [71]–[73]	the reaction of light absorbed and reflected on the surface of the skin on the regions of interest	forehead [71], [72], cheek [72], hand palm [71]–[73]	PTT (with ECG) [71], PTT with Distal Signal (PPG or VPG) [72], relationship between the internal pressure and the cross-sectional area of the blood vessel [73]	non-contact; can be used in remote health monitoring in hospitals, elderly homes, workplaces, and drivers	External light adds noise to data; equipment needs to meet certain requirements; user's position must be precise, stationary poses, not ideal for long-term monitoring
Ultrasound [77]–[80]	deriving blood velocity, blood volume flow, blood vessel's wall thickness, and diameter waveforms from a probe against region of interest	carotid artery [77]–[80]	PWV [77], [79], force sweep [78], Doppler [80]	carotid artery provides strong central diastolic BP and systolic BP; PWV more accurate than PTT acquisition	angle, pressure, calibration inaccuracies can lead to issues with data acquisition, not wearable, needs medical training for accurate readings
Magnetic Plethysmography (MPG) [74]–[76]	detecting fluctuations caused by blood flow in an ambient magnetix field encompassing the blood vessel	carotid artery [74], [76], middle finger of left hand [75]	PWV [74]–[76]	less affected by optical and biological characteristics of living tissue, wearable applications	signal not investigated thoroughly such as PPG

PTT = Pulse Transit Time, SNR = Signal to Noise Ratio, PWV = Pulse Wave Velocity, ECG = Electrocardiogram

This article has been accepted for publication in a future issue of this journal, but has not been fully edited. Content may change prior to final publication. Citation information: DOI 10.1109/ACCESS.2020.3040257, IEEE Access

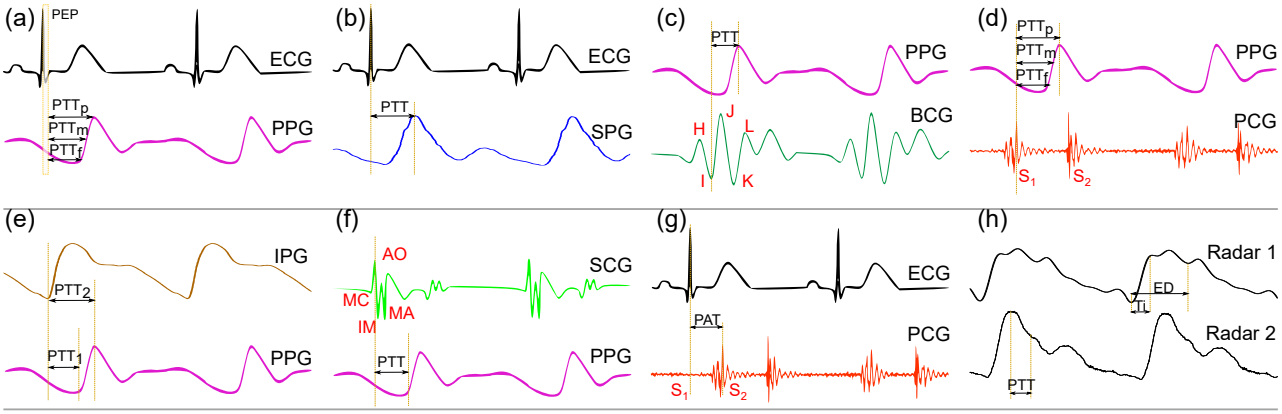

FIGURE 6: Key features for BP estimation using different physiological signals: (a) Using the R-peak of ECG signal and PPG signal's peak and its derivative; (b) Using the R-peak of ECG signal and SPG signal's peak; (c) Using BCG signal and PPG signal; (d) Using PPG signal and PCG signal; (e) Using IPG signal and PPG signal; (f) Using SCG signal and PPG signal; (g) Using ECG signal and PCG signal; (h) Using two Radar signals.

however, the sensor placement and exposure to lighting can drastically affect accuracy. Additionally, the authors in [22] stated that this method is not robust enough to calculate DBP. The authors in [23] proposed a solution to derive both SBP and DBP from PTT as well as test the limits of using this method relative to motion artifacts. Linear regression was applied to the PTT correlation between 3 channels of ECG and 1 channel of PPG for continuous BP estimation on 14 subjects in five positions (recumbent, seated, standing, walking, cycling). The results demonstrate the abilities of the proposed architecture and reported a lower correlation function SBP mean and standard deviation for stationary positions such as sitting (0.07 ± 5.8 mmHg) with an increase in positions with motion like walking and cycling (4.4 ± 20.9 mmHg and 10.2 ± 16.0 mmHg respectively) [23].

Another ECG dependent method includes SPG. ECG is measured via sensors on the chest of the subjects and compared in real time to SPG and PPG. The studies investigating SPG in vitro have shown an improved SNR and robustness to motion artifacts and temperature tests compared to PPG, where the latter produces noisy waveforms [52], [53].

ECG is also demonstrated to be useful in radar BP systems [67]. In a radar BP system with contact, an antenna is attached to the subject, typically the sternum to acquire the arterial pulsation from the aortic arch. [67] includes this in their system paired with bioimpedance and ECG electrodes to accurately measure PTT and PAT during exercise. From the arterial pulse across the carotid and subclavian arteries and a bipolar lead from ECG, PTT is calculated over the central elastic arteries, reducing changes in the measurement from vasomotion produced in peripheral arteries. The system is successful in estimating BP at the central proximal arteries without a cuff, and the sensors can be hidden under clothes [67]. However, this system can be uncomfortable for users to wear for long term testing and is susceptible to issues regarding electrodes on the body such as adhesiveness to the skin.

ECG in VPG systems are used for PTT measurements [71]. By capturing areas on the face and/or hand, cuff-less BP can be derived with VPG in different methods. One technique includes using ECG to calculate PTT between the R peak of the ECG signal and the foot of the VPG signal in the forehead. The forehead VPG signal is used as the SNR is higher relative to the palm [71]. Using PTT from ECG and VPG on three subjects, [71] demonstrated total absolute mean error and standard deviations of 9.48 ± 7.13 mmHg and 4.48 ± 3.29 mmHg, for SBP and mean arterial pressure respectively.

ECG signal used as a proximal waveform also is combined with IPG signal. Liu et al. [85] designed an IPG ring that, when recorded simultaneously with an ECG signal, was able to estimate BP through the PTT method. The PTT interval in this experiment was defined as the time delay between the R peaks of the ECG signal and the peaks of the IPG signals. The obtained results showed that the change of SBP had a better relationship with the change of the PTT induced by IPG than that of PTT derived by PPG signal and ECG signal, forming the Pearson correlation coefficients of 0.700 and 0.45 respectively.

2) Using BCG as a proximal waveform

BCG is also known to be closely correlated with arterial BP [30]. Thus, many studies have working on deriving BP measurements through the BCG's combination with other physiology signals such as ECG, PPG, and others. Kim et al. [86] proposed a method based on PTT to estimate BP through BCG signals collected by a scale-like platform. In this study, the time difference between proximal and distal sites are considered as the time interval between BCG and a non-invasive measured finger BP waveform. Yousefian et al. [32] developed a wristband with built-in BCG and PPG sensor to investigate the potential of wearable BCG to enable cuff-less BP monitoring. The authors create a PTT method

which both the BCG and PPG signals are acquired by a wristband as proximal and distal timing reference (Fig. 6c). The result reveals that BP estimated through a wrist PTT is close to both SBP and DBP with the mean absolute error of 5.1 mmHg and 7.6 mmHg respectively. While doing thorough research about the BCG signal's morphology, C. Kim et al. [87] presented an association between the J-K amplitude and PTT, enabling independent monitoring of SBP and DBP via the J-K amplitude. A chair-based platform used for BP monitoring was proposed by [33]. Two BCG signals are measured through sensors located in chair's back and seat plates. The authors then extract an instantaneous phase different (IPD) as a feature to estimate BP. The result shows that IPD could estimate more accurate readings of BP compared to PTT.

3) Using PCG as a proximal waveform

Since the variation in the cardio hemodynamic is reflected directly on various physiological signals, including the PCG signal, several attempts have been made to estimate BP through PCG signal. Shukla et al. [88] proposed a new approach to measure BP using vascular transit time (VTT), defined as the time interval between S1 and the peak of a PPG signal. The authors conducted an experiment on 7 subjects and yielded the accuracy of 95% compared with reference BP. With the same approach, Hsiao et al. [89] designed an auscultation sphygmomanometer that continuously monitors both PCG and PPG, aiming to estimate BP. The study shows that the error in SBP is 6.67±8.47 mmHg for the range of normal BP. Esmaili et al. [90] presented an approach with the PTT method using PCG and PPG signals simultaneously (Fig. 6d). The obtained results are promising as the correlation coefficients were equal to 0.89 and 0.84 for SBP and DBP respectively. A correlation between PTT derived directly from a reference BP and both systolic (S12) and diastolic (S21) duration, the SBP and DBP are then calculated by the value of PTT [91]. The results are very close to the Association for the Advancement of Medical Instrumentation (AAMI) standard and listed in the summary, Table III.

4) Using SCG as a proximal waveform

As described in Section II.A, SCG holds great potential for cNIBP. Carek et al. [92] proposed a wearable device, named SeismoWatch, as shown in Fig.7a, that can obtain a low root mean square error of 2.9 mmHg for DBP. Specifically, the authors developed a wrist-watch BP monitor with simultaneous recordings of PPG and SCG. The watch was held against the sternum to detect micro-vibrations (SCG signal) and the travel time (PTT) was measured by the time delay between the AO and PPG signals (Fig. 6f). A smartphone-based BP monitoring application was presented in [45] with the use of SCG and PPG simultaneously recorded by the built-in smartphone accelerometer and camera respectively. The PTT interval calculated as the time delay between AO and the wavefront of the PPG signal and was utilized to estimate

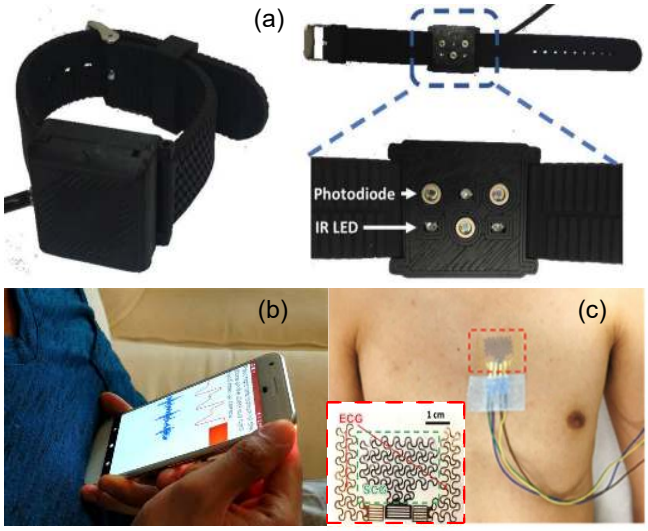

FIGURE 7: cNIBP using SCG waveforms: (a) A wrist-watch BP monitor with PPG sensor and accelerometer sensor embedded. Image courtesy of Carek et al., [92]; (b) Smartphone-based BP monitor. Adopted from [45]; (c) An ultrathin and stretchable E-tattoo simultaneously measure ECG and SCG for BP. Adopted from [93].

the BP. While one finger covers the camera to collect PPG, a user holds the phone and press it on the left side of the chest to record SCG as described in Fig.7b. The study showed the Pearson correlation coefficient of BP across participants between 0.20 and 0.77 with an RMSE of 3.3±9.2 mmHg for DBP. A recent study [93] leveraged electronic advancements to develop an ultrathin and stretchable e-tattoo for SCG sensing and BP measurement (Fig.7c). The study showed the correlation between SBP and DBP with the RAC interval (i.e., time interval between R peak of ECG and AC point of SCG) with the coefficient of -0.772 and -0.858 respectively.

5) Single Waveform-Based Methods

While many techniques utilize two different waveforms (i.e., proximal and distal waveform) at different body's locations in their PTT methods, there are some emerging methods that use one type of waveform from different ROIs to form PTT. Authors in [68] reported a non-contact 2.45 GHz quadrature Doppler radar system to track chest displacements from cardiac motion in order to derive pulse pressure with carotid-femoral PTT (cf-PTT). Using the waveform reflected from the subject, the signal is filtered using arc-tangent demodulation for absolute displacement, which can be used regardless of distance between the user and the device [68]. From sitting and laying down at a fixed distance from the radar, two subjects were used to validate the technique and were successful in measuring cardiac motion within millimeters of accuracy. In spite of this, the proposed architecture needs to be individually calibrated to provide accurate results and the orientation between the device and user must be considered. Another non-contact Doppler system is used in [69]; however, static

and beat-to-beat SBP and DBP are measured from capturing the vasomotion of the central aortic artery to calculate cf-PTT. This value is calculated from the difference of the ejection duration of the cardiac pulse and the first systolic peak (Fig. 6). The architecture of the device comprises a pair of antenna arrays, a frequency synthesizer, and a digital-IF receiver. From the calculated cf-PTT, the static BP errors are within 3 mmHg, and the beat-to-beat BP measurements are about 98% accurate [69]. This device has less flexibility than [68] in regards to subject position and radar distance from ROI, but it does not require individual calibration.

With only PPG signals simultaneously collected at different locations in the body, there are some attempts to predict BP. Tabei et al. [82] used two PPG signals collected by two identical smartphones in two hands. The PTT, which was previously defined as the time taken for the blood to travel between the proximal and distal arterial sites, was then calculated as the time interval between two peaks of two PPG signal. The error for systolic blood pressure (SBP) and diastolic blood pressure (DBP) estimation is 2.07 ± 2.06 mmHg and 2.12 ± 1.85 mmHgrespectively, which achieved the AAMI/ISO standard criteria for BP measurement. Another study [84] presented the use of a PPG sensor at multiple wavelengths for BP measurement. The authors revealed arteriolar PTT (i.e., time difference between the pulse wave arrivals in the capillary and arterial layers) achieved higher performance than the arterial PTT method.

Another single waveform-based method is a wrist-worn device that records two IPG signals was proposed by Huynh et al. [66] to estimate the BP. The authors characterized various distances between two IPG signals, and the different PTT intervals were calculated by the time differences between the peak, middle, and foot points of the IPG waveforms (Fig. 5b). The group average correlation coefficients and RMSE between SBP and DBP from the proposed device and the standard device was listed in the Table III. Likewise, the authors presented another wearable device that estimate BP through IPG and PPG recorded simultaneously in the finger [44] (Fig. 5c). In this study, they calibrate the time difference between two sensors due to a small distance between the wrist and the finger, inducing a different phase shift. This prevents the PTT value from being significantly fluctuated. The results are slightly improved in terms of the correlation coefficient compared with their previous work in [66].

An additional single waveform-based approach is the perpendicular US velocimetry (PUV) approach which samples raw radio-frequency-data frames using high frame rate and particle image velocimetry, creating a dataset of high precision 2D or B-Mode velocity vectors [77]. The perpendicular element of US allows for tracking diameter changes in the blood vessel while simultaneously measuring flow, pressure waveforms, and local PWV in large arteries, which was unable to be realized with Doppler US techniques. PWV, a reciprocal value of PTT, is calculated using the flow-area (QA) method, which measures PWV from the ratio between the change of flow and the change in cross-sectional area. Using a phantom vessel submerged in water, [77] validated the QA method with the resulting waveform being a variation of 0.3 m/s from the reference PWV; however, this method increases in inaccuracy with reflections in the data, non-uniformed tissue around the vessel, and limited computation of device.

MPG can calculate BP through just its waveform by utilizing a pair of probes embedded with transducers to calculate local arterial PWV. Chandrasekhar et al. [74] proposed a single and a dual element probe design using a Giant Magneto Resistance sensor to create an electromagnet based MPG transducer. The single MPG transducer was validated in-vivo testing of carotid to radial artery PWV against an occlusion test while the dual element MPG transducer is proposed to measure PWV in 15mm sections of the artery. Later, the same research group presented an arterial compliance probe with dual MPG transducers for non-invasive BP monitoring [75]. The transducers were placed 23mm apart in the probe and were composed of Hall-effect sensors and permanent magnets. Using 20 subjects with a phantom artery as reference, the method was tested on the carotid artery before and after exercise while the users were at rest. This resulted in a Pearson correlation coefficient of r= 0.72 between the local PWV and the Brachial BP reference and a lower correlation for pulse pressure (r = 0.42). Another method for MPG uses a finger cuff for measurement [76]. This is performed by using time varying magnetic fields and monitoring the change of impedance from the exciting coil, which is related to the change of blood volume in the ROI. Compared to a US Doppler blood flow velocity recording, the authors report Pearson correlation coefficients of r = 0.9355 and $p < 0.01$.

Using only distal waves, a bi-modal probe combining a US probe and 2 PPG sensors is introduced in [79] and demonstrates the ability to measure diameter values and local PWV of the carotid artery with distal waveforms, resulting in real-time carotid BP without prior calibration using subject or population-specific parameters. To achieve a calibration free technique, the US probe reports the difference in the SBP and DBP as well as the DBP while the two PPG sensors calculate the local PWV and feed these results into the P–β model in [79]. The absolute error compared to a brachial-based cuff for carotid DBP was less than 10 mm-Hg in 82% of the 83 subjects, non-hypertensive and hypertensive, while the SBP was lower than the reference [79]. Further testing with a catheter reference may give more accurate results for the success of this method.

Lastly, apart from those using VPG and another waveform (e.g., ECG) to derive BP, some have carried approaches reliant only on VPG. Nitzan et al. [94] utilized a parameter, specified as PTTD (PTT using only distal signals), which is the PTT difference between VPG pulse arrival to a toe and finger. However, the resulted VPG signals were prone to noise and motion artifacts. In parallel, authors in [72] used only one VPG from a ROI to calculate BP without PTT. A single VPG signal was recorded and processed with a bandpass filter and linear fitting, making two variations of

the signal, and forming an index, T_{bh}, from the difference in the minimum points. This technique demonstrates a higher performance with VPG measured from the right palm rather than from the forehead or right cheek due to noise from the nervous system in the face [72]. PTTD between the two VPG signals resulted in PTT and SBP correlation coefficients (-0.6045$\pm$0.0399), which are lower compared to the first method (-0.7163$\pm$0.0761) [71].

IV. DISCUSSION

This review aims to provide highlights of technologies using PTT/PAT as the parameter to derive continuous, non-invasive cuff-less blood pressure. There are numerous combinations between two signals or multiple signals that have been utilized to acquire PTT/PAT. However, several aspects (e.g., transmission distance and the starting and ending points of the time delay) should be taken into account to achieve high accuracy for enabling cNIBP monitoring. To the best of our knowledge, a combination between ECG and PPG signals is the most commonly-used pair to derive PTT/PAT value. The starting point of the time delay is the R-peak of ECG, while the ending point varies from the peak of PPG to the first/second derivative of the PPG signal. As aforementioned the PTT and PAT values are interchangeably used for time delay between two signals. However, with the pre-ejection period (PEP) included, it should be careful to choose either PTT or PAT for BP estimation as it may vary the accuracy of each method [2].

cNIBP techniques have varying levels of success depending on the reliability of the signal, noise level, sensor placement, wave propagation, calibration, and evaluation parameters. The two biggest challenges to make cNIBP practical have been determined as the need for frequent calibration as well as the susceptibility to motion artifacts of electrophysiological signals in the daily life. The reliability of a method is validated with thorough testing scenarios, amount of data, and the gold standard for comparison. The noise level, typically quantified as SNR, also factors into the reliability of the signal morphology and refers to the motion artifacts that can affect the signal quality, such as other biosignals and motion from the body. Sensor placement is another key component in signal reliability since the sensor must be able to obtain blood pressure while considering the physics and biology of the region of interest. The wave propagation theory used has these physiological conditions factored into the equation or results, and the sensor may require calibration to reflect these constraints correctly. The evaluation parameters quantify how reliable the signal is in acquiring cNIBP.

Based on their abundance of use in literature, the most prominent proximal and distal waveforms in PTT/PAT-based cNIBP development are ECG and PPG. Many have used ECG or PPG in the PTT equation or as a reference signal for evaluation parameters, as demonstrated in Table 3. The widespread use of these signals is due to their inexpensive setup. ECG, in particular, has a very informative waveform, showing the P wave, QRS complex, and T wave, and is a reliable method for R-wave detection [9]. While they are the most commonly used in cNIBP approaches, they also have drawbacks that make them unreliable. The PPG signal can become affected by noise in cold and/or bright environments [53]. ECG also needs to be paired with another signal to derive SBP and DBP accurately [21]–[23]. For example, SPG has the potential for being a good replacement for PPG as it has better SNR and can provide a strong signal in tests under low-temperature environments.

Since PTT is a relative parameter that correlates with BP, the method needs calibration to calculate the absolute value of blood pressure [3], [96]. In other words, the calibration process is needed to precisely choose different parameters for the model and to find the relationship between the actual BP and the PTT measurements over a wide range of BP values [2]. There have been numerous methods (e.g., physical exercises, valsalva maneuvers, and cold pressor) deployed that would perturb an individual's BP and resulted in large variations of BP values induced by a set of interventions [9]. Regarding the BP perturbance-induced method, several aspects of calibration should be cogitated, such as the calibration process, calibration frequency, and whether the process is done by population or individuals. For instance, calibration can be conducted either one-time at the beginning or periodically throughout a period. The main drawback of one-time calibration is not to provide a large enough range of reference BP value. This may result in inaccurate BP calculation during extreme cases (e.g., hypertension or hypotension). Although periodical calibration improves accuracy, it may cause inconvenience to users.

Regarding database availability, although numerous studies have worked on cNIBP, there are few publicly available databases. The first database is the Multiparameter Intelligent Monitoring in Intensive Care (MIMIC) Database [97]–[99], which contains thousands of recordings simultaneously collected on the patients. Each set of databases includes multiple physiological signals such as PPG signals, ECG signals, and arterial blood pressure (ABP) at a sampling frequency of 125 Hz. Several papers [100]–[102] have used the MIMIC database to derive PTT values. It should be noted that the PPG and ECG signals are not perfectly synchronized since they are collected from multiple sources and electronic hardware, and additional time delays could be included, leading to erroneous conclusions [103]. Another recently published database [104], named PPG-BP, contains 657 data segments from 219 subjects, between the ages of 21 and 86 years. The database includes PPG signals collected along with BP readings. The database covers several diseases such as hypertension, diabetes, cerebral infarction, and insufficient brain blood supply. Since only PPG signals are recorded with BP readings, the PTT/PAT-based method for BP measurement is barely applicable as it requires at least two signals recorded in two separate sites of the body. However, this database still holds potential value for further investigation in using PPG signal as a surrogate of BP measurement, especially with pulse wave analysis that relies on the crafted features of a

TABLE 3: PTT-based BP measurement

#	Sensors	Parameters Measured	Activities	Error±Standard Deviation in mmHg			Pearson coefficient	Ref.
				SBP	DBP	MAP		
22	BCG+PPG	PTT(from I and J wave collected in wrist to the foot of PPG wave)	Cold pressor, metal arithmetic, slow breathing and breath holding	7.6[1]	5.1[1]	N/R	0.81 SBP and 0.79 DBP	[32]
22	BCG+PPG +ECG	PTT(from I wave of BCG to the foot of PPG wave)	Metal arithmetic, cold pressor and post-exercise state	7.3[2]	5.7[2]	N/R	0.8 SBP and 0.87 DBP	[87]
15	BCG +finger cuff	PTT(from I wave of BCG to the peak of BP collected by a finger cuff)	Deep breathing and sustained hand grip	130.2±16	89.5 ±11.11	105.1 ±11.8	0.65±0.15 SBP and 0.60±0.17 DBP	[86]
15	IPG*2	PTT(from the peak of IPG 1 to the peak of IPG 2)	Handgrip exercise	7.3±2.15[2]	5.17±1.81[2]	N/R	N/R	[66]
15	IPG+PPG	PTT(subtraction between PTTc obtained when two sensors at the same place and PTTm obtained when two sensors apart)	Handgrip exercise	8.47±0.91[2]	5.02 ±0.73[2]	N/R	0.88±0.07 for SBP and 0.88±0.06 for DBP	[44]
20	IPG+ECG	PTT(from the R peak of ECG to the peak of IPG)	Cycling	N/R	N/R	N/R	0.727 for SBP and 0.332 for DBP	[85]
32	PCG+PPG	PTT(from the S1 of PCG to the peak/first derivation/second derivation of PPG)	Physical exercise	6.22±9.44[1]	3.97±5.15[1]	N/R	0.89 for SBP and 0.84 for DBP	[90]
85	PCG+PPG	VTT(from the S1 of PCG to the peak of PPG)	Stretch arms	6.67±8.47[1]	N/R	N/R	N/R	[89]
4	SCG+ECG	RAC(from the S1 of SCG to the peak of ECG)	Valsalva maneuver - Exhalation with close noise and mouth every 30s	N/R	N/R	N/R	-0.772 for SBP and -0.858 for DBP	[93]
10	SCG +acoustic sensor	PTT(from the AO of SCG to the peak of acoustic waveform)	Valsalva maneuver and sustained hand grip	N/R	N/R	N/R	0.58±0.14 for SBP and 0.57±0.13 for DBP	[95]
9	SCG+PPG	PTT(from the AO of SCG to the foot of PPG)	Stationary biking with different intensities	N/R	3.3±9.2	N/R	N/R	[45]
13	SCG+PPG	PTT(from the AO of SCG to the foot of PPG)	Cold pressor	N/R	2.9[1]	N/R	N/R	[92]
25	ECG+PPG	PAT(R peak of ECG and peak of PPG)	N/R	7.77	4.96	N/R	N/R	[21]
23	ECG+PPG	PTT(R-wave of ECG to PPG)	N/R	-0.3±3.1	N/R	N/R	BP SMM and BP PTT was 0.983	[22]
14	ECG+PPG	PTT(R peak of ECG and peak of PPG)	recumbent, seated, standing, walking, cycling	N/R	N/R	N/R	N/R	[23]
6	Radar+ECG +Bioimpedence	PTT(Rising Slope in BioImp and the max 2nd derivative of Radar)	exercise on a bicycle	N/R	N/R	N/R	-0.48 (p=0.0029)	[67]
3	CW Doppler Radar	carotid-femoral PTT from the central aortic pulse wave	N/R	3±120	3±76	N/R	N/R	[69]
3	VPG+ECG	PTT(R peak of ECG and foot of VPG)	post-exercise (running)	9.48±7.13	N/R	4.48±3.29	-0.7163±0.0761 ($p<0.05$)	[71]
83	US+PPG*2	PWV (Distance from US, Time delay from PPG peak differences)	N/A	N/A	N/A	N/A	$p<0.05$	[79]

Abbreviations: # = number of subjects, ECG = Electrocardiogram, IPG = Impedance plethysmography, PCG = Phonocardiogram, BCG = Ballistocardiograph, PPG = Photoplethysmogram, SCG = Seismocardiogram, VPG = Videoplethysmogram, US = Ultrasound, MPG = Magneticplethsmogram, AO = The aortic valve opening (AO) in the SCG signal, PTT = pulse transit time, PWV = Pulse Wave Velocity, N/R = not reported, SBP = systolic BP, DBP = diastolic BP, MAP = mean arterial pressure, [1] = MAE (mean absolute error BP), [2] = RMSE (root mean square error BP).

single PPG waveform.

In terms of evaluation methods, metrics such as Pearson correlation coefficient, ME, MSE, and RMSE are commonly used in justifying the success and accuracy of a signal. Many papers reviewed in Section II.C and II.D use these metrics to evaluate the experimental results, as reported in Table 3. Although these metrics are used to compare with each gold standard presented in each experiment, the numbers cannot be translated to evaluate various methods across different researches due to different gold standards, experimental setups, and databases. Standardization of such methods can make comparisons between signals and methods much more straightforward. This is a challenge since the developed techniques have different conditions and parameters to check, making regulating difficult to perform. Using a base check, such as recording subjects at rest before exercising with the device, then comparing to data from open-access databases and inferring some correlations, can help with this effort; however, there are still gaps of knowledge that require further investigation to examine methods accurately. To bridge this gap, machine learning may have the potential to discover more correlations that PTT/PAT-based methods are not able to infer.

A discrepancy discovered through this review is the number of patients used to validate methods varies greatly among papers ranging from two to three subjects to over a hundred (see Table 3). This makes comparing methods, even ones using the same signal to derive cNIBP, difficult since each group has different testing conditions and levels of completeness for their project (i.e. prototype and clinical-grade products). Methods using more subjects can address a wider range of features presented in a larger sample population and thus could provide better accuracy for home-based applications of cNIBP. However, when comparing the Pearson coefficient values in reported literature, there are no noticeable differences amongst methods with a high number of subjects versus a few. The real evaluation of these methods needs to be obtained through a different method to ascertain how effective the proposed methods will be in the daily life.

V. FUTURE DIRECTIONS

PTT/PAT-based BP measurement is currently an active area of research, and many groups have developed methods that may help not only improve the accuracy of future PTT/PAT-based cNIBP, but also actualize this concept to be applicable in reality. In this session, we provide some anticipation and recommendations for cNIBP monitoring in general and PTT/PAT-based methods in specific, with the concentration on 1) measurement techniques improvement; 2) deep learning-based BP estimation and signal de-noising with single-site measurements; 3) the application of cNIBP on medical research; 4) experimental setup, protocol development, and validation procedure.

Measurement instrumental and algorithmic enhancement: As aforementioned, ECG is the most commonly used signal in the PTT/PAT-based BP monitoring. With the use of conventional electrodes, such as Ag/AgCl electrodes, it usually causes skin irritation and discomfort [24]. Moreover, ECG is measured from the potential between two electrodes across the two sides of the heart by long wire connected to acquisition, which is not conveniently wearable. To address this issue, non-contact electrodes (NCE) integrated in a portable ECG device are an alternative solution, which possesses some advantages: 1) it is immune to signal degradation for long-term measurement; 2) it reduces setting up time and increases the ease of use as it does not require skin preparation [24].

Collecting multiple signals for the PTT/PAT-based measurement is sometimes cumbersome, which mostly stems from the unwieldiness of hardware setup and the inconsistency of signals during the measurement. A potential solution is to use only easily-obtainable signals like PPG to precisely infer signals that require bulky setup like ECG, given that both types of signals are directly synchronized with human cardiac cycles. In [105], a machine learning-based approach was proposed to estimate ECG parameters and the ranges of RR, PR, QRS, and QT intervals based on the extracted time and frequency domain features from a fingertip PPG signal. The method achieved a 90% accuracy on a benchmark hospital dataset having clean PPG signals. Furthermore, the authors in [106] proposed a signal model to linearly reconstruct the entire ECG from PPG waveforms. The method reached a subject-wise accuracy of 98% in averaged correlation on a benchmark dataset of subjects with different ages and weights. Nevertheless, the method still has reconstruction deficiencies in subject independent modes and does not take into account the PTT. Therefore, rigorous evaluations on a wide range of ECG morphologies and abnormalities in real-world settings, as well as evaluations that consider the inferred PTT, are necessary. The success of this research direction will further enable low-cost blood pressure measurement for continuous and long-term monitoring.

Deep learning based BP estimation and signal denoising with single-site measurements: Over the past few years, the deep learning field [107] has witnessed tremendous advancements due to data availability, computational resources, and better training algorithms. Deep neural networks achieved state-of-the-art performance in a wide range of tasks, including image classification, audio synthesis, and machine translation. Deep learning adapts to represent hierarchical features at multiple network layers by the composition of lower-level features into higher-level representation. It automatically learns a complex function approximator to map raw data inputs to desired outputs directly. With the expressiveness of deep learning, several recent studies have been proposed to estimate BP with cuffless devices using only a single measurement, such as PPG, without depending on hand-crafted features. In [108], an end-to-end approach is proposed to estimate blood pressure from the pulse wave signal. Without complicated feature extraction, a normalized single pulse wave is fed into a deep neural network, which consists of depth-separable convolutional layers and gated

recurrent units in the recurrent layers. Their approach is able to achieve the average absolute systolic BP error of 3.95 mmHg and the average absolute diastolic BP error of 2.14 mmHg on the MIMIC dataset. Similarly, Slapnvicar et al. [109] proposed a deep learning method that takes into account both temporal and frequency information contained in the PPG waveform and its derivatives. The novel spectro-temporal residual neural network attains mean absolute errors of 9.43 for systolic and 6.88 for diastolic BP on the MIMIC-III dataset.

Additionally, deep learning can be applied to improve signal quality. In real-world scenarios, the aforementioned measurements are susceptible to various noises, such as baseline wander, muscle artifact, and electrode motion, which poses the need for effective noise-reduction methods. In [110], a bidirectional recurrent denoising auto-encoder model is proposed to not only denoise PPG but also provide waveform feature accentuation. Its performance on a large open database of noise-augmented PPG improves signal-to-noise ratio by 7.9 dB. Chiang et. al. [111] proposed a fully convolutional autoencoder to denoise ECG. This is tested on noise-added ECG signals from the MIT-BIT Arrhythmia database. With an input SNR of -1 dB, the model can improve signal-to-noise ratio by 15.49 dB.

Importantly, with the latest advances to make deep learning models more transparent by interpreting their decisions [112], [113], these methods will become more trustworthy and better adapted to clinical settings.

Applying cNIBP to uncover the relation between blood pressure and infectious diseases: Recent advances in machine learning and low-power wearable medical devices have enabled remote and automated diagnoses via continuous physiological monitoring. For instance, Jeong et al. [114] suggested that the onset of COVID-19 in individuals could be detected through continuous on-body sensing. Detecting infectious diseases with non-invasive sensing is advantageous over lab examinations (e.g., RT-PCR, and immunoassays) in at least two aspects: safety and scalability. As the predictive model matures, public health authorities can benefit from the widespread availability of non-invasive health sensor signals, including the recent addition of cNIBP.

Nevertheless, challenges need to be overcome to make on-body sensing practical for COVID-19 detection. The most critical one is to design soft-electronic sensors that can be intimately attached to the skin without irritable reactions [114]. According to Mueller et al. [115], COVID-19 is 23× more likely to lead to death in cohorts older than 65 years old. The fragiliy of elderly skin adds an additional constraint to the sensors. The PDMS-based tonometric BP sensors designed by Kim et al. [116], and Huang et al. [117] both addressed skin conformity and non-irritability.

It is still an open research question on whether (high) blood pressure has an effect on the progression of COVID-19 infection. Kario et al. [118] highlights that patients with hypertension are known to have higher risks to develop severe symptoms during COVID-19 infection. However, it is still unclear whether hypertension (or its medication such as Renin-angiotensin-aldosterone system (RAAS) inhibitors [119]) is a direct cause to the exacerbation of COVID-19 symptoms. We hope the wider availability of cNIBP sensors can shed lights on these medical inquiries.

Usability, acquisition techniques, and experimental standards improvements: As garnered from this review, there are an abundant amount of methods using PTT, PAT, or PWV-based calculations to estimate SBP and DBP non-invasively. This includes experimental setups using only one type of signal (e.g., two PPG signals or two VPG signals) or a hybrid of proximal and distal signals (e.g., PPG and ECG). Many of these techniques are developed into or are in the process of being adapted into cuff-less wearables that will make continuously measuring blood pressure more feasible in remote and home-based healthcare. However, in order for this vision to be fulfilled, future research in this field needs to center around creating devices that address the following suggestions:

1) The product must be user-friendly in design (e.g., wearable and small).
2) To use the device accurately, no complex medical training is needed.
3) The recorded blood pressure must account for motion artifacts from daily life (e.g., walking and working) and be able to filter out this noise in the acquired signal.
4) To improve accuracy, investigate using more than 2 sensors as well as different distal signal configurations.
5) More regions of interests need to be investigated for each signal (e.g., many PPG sensors configurations record predominately at the finger while using a leg is possible and potentially more advantageous).
6) The experiments need to include more a more substantial amount of tests subjects (e.g., greater than 50) that are diverse in age and with health conditions (e.g., hypertensive or pregnant).
7) The gold standard for verifying blood pressure acquisition needs to be more uniformed between experiments (e.g., use invasive method such as volume clamp to confirm results).
8) Integrate these devices with smartphones for recording blood pressure and facilitating better incorporation into consumer life.

VI. CONCLUSIONS

In this article, we reviewed 1) various sensor technologies that enable cNIBP monitoring and 2) recent state-of-the-art approaches related to PTT/PAT-based BP estimation. From the proximal and distal waveforms, we highlight the pros and cons of different signal combinations that could derive PTT or PWV information in cuff-less settings. Using PTT or PWV reveals the importance of considering the pre-ejection period, the physical properties of the artery, and the physiological factors of the user to obtain accurate hemodynamic estimations. Additionally, this review also addresses different technical challenges, such as the need for frequent calibration

and the susceptibility to motion artifacts, that all need to be overcome before PTT/PAT-based methods can be readily applied to routine diagnosis procedures. Furthermore, the lack of large scale cNIBP datasets creates an additional barrier for data scientists who crave to develop general signal processing algorithms. We have determined limitations of wave propagation methods, signal-to-noise ratio, and calibration issues can be addressed by machine learning methods. In brief, future breakthroughs of cNIBP monitoring will most likely call for collaborative efforts from biomedical engineering, computer science, electrical engineering, and medical disciplines. We are hopeful that home-based, intelligent, and continuous BP monitoring would be achieved in the near future. Through advancements of cNIBP sensing, the cost of care can be significantly reduced, and our patients' quality of life could be greatly.

REFERENCES

[1] K. Bartels, S. A. Esper, and R. H. Thiele, "Blood pressure monitoring for the anesthesiologist: A practical review," *Anesthesia and Analgesia*, vol. 122, no. 6, 2016.

[2] S. Josep and R. Delgado-Gonzalo, *The Handbook of Cuffless Blood Pressure Monitoring: a Practical Guide for Clinicians, Researchers, and Engineers*. Springer, 2019.

[3] M. Sharma, K. Barbosa, V. Ho, D. Griggs, T. Ghirmai, S. K. Krishnan, T. K. Hsiai, J.-C. Chiao, and H. Cao, "Cuff-less and continuous blood pressure monitoring: A methodological review," *Technologies*, vol. 5, no. 2, p. 21, 2017.

[4] A. Valderrama, C. Gillespie, S. King, M. George, and Y. Hong, "Vital signs: Awareness and treatment of uncontrolled hypertension among adults — united states, 2003–2010," *MMWR. Morbidity and mortality weekly report*, vol. 61, Sep. 2012.

[5] "Ieee standard for wearable cuffless blood pressure measuring devices," *IEEE Std 1708-2014*, pp. 1–38, 2014.

[6] S. i. Carós and J. i. Maria, "Continuous non-invasive blood pressure estimation," Ph.D. dissertation, ETH, 2011.

[7] D. Perloff, C. Grim, J. Flack, E. D. Frohlich, M. Hill, M. Mcdonald, and B. Z. Morgenstern, "Human blood pressure determination by sphygmomanometry.," *Circulation*, vol. 88, no. 5, pp. 2460–2470, 1993.

[8] J. C. Bramwell and A. V. Hill, "The velocity of pulse wave in man," *Proceedings of the Royal Society of London. Series B, Containing Papers of a Biological Character*, vol. 93, no. 652, pp. 298–306, 1922.

[9] R. Mukkamala, J. Hahn, O. T. Inan, L. K. Mestha, C. Kim, H. Töreyin, and S. Kyal, "Toward ubiquitous blood pressure monitoring via pulse transit time: Theory and practice," *IEEE Transactions on Biomedical Engineering*, vol. 62, no. 8, pp. 1879–1901, 2015.

[10] E. G. Lakatta and D. Levy, "Arterial and cardiac aging: Major shareholders in cardiovascular disease enterprises," *Circulation*, vol. 107, no. 1, pp. 139–146, 2003. eprint: https://www.ahajournals.org/doi/pdf/10.1161/01.CIR.0000048892.83521.58.

[11] R. H. Cox, "Regional variation of series elasticity in canine arterial smooth muscles," *American Journal of Physiology-Heart and Circulatory Physiology*, vol. 234, no. 5, H542–H551, 1978, PMID: 645919. eprint: https://doi.org/10.1152/ajpheart.1978.234.5.H542.

[12] G. Chan, R. Cooper, M. Hosanee, K. Welykholowa, P. A. Kyriacou, D. Zheng, J. Allen, D. Abbott, N. H. Lovell, R. Fletcher, and M. Elgendi, "Multi-site photoplethysmography technology for blood pressure assessment: Challenges and recommendations," *Journal of Clinical Medicine*, vol. 8, no. 11, 2019.

[13] G. Zhang, M. Gao, D. Xu, N. B. Olivier, and R. Mukkamala, "Pulse arrival time is not an adequate surrogate for pulse transit time as a marker of blood pressure," *Journal of Applied Physiology*, vol. 111, no. 6, pp. 1681–1686, 2011, PMID: 21960657. eprint: https://doi.org/10.1152/japplphysiol.00980.2011.

[14] Parry Fung, G. Dumont, C. Ries, C. Mott, and M. Ansermino, "Continuous noninvasive blood pressure measurement by pulse transit time," in *The 26th Annual International Conference of the IEEE Engineering in Medicine and Biology Society*, vol. 1, 2004, pp. 738–741.

[15] R. Mukkamala, J.-O. Hahn, O. T. Inan, L. K. Mestha, C.-S. Kim, H. Toreyin, and S. Kyal, "Toward ubiquitous blood pressure monitoring via pulse transit time: Theory and practice," *IEEE Transactions on Biomedical Engineering*, vol. 62, no. 8, pp. 1879–1901, Aug. 2015.

[16] A. Stojanova, S. Koceski, and N. Koceska, "Continuous blood pressure monitoring as a basis for ambient assisted living (aal) – review of methodologies and devices," *Journal of Medical Systems*, vol. 43, no. 2, Jan. 2019.

[17] D. M. Bard, J. I. Joseph, and N. van Helmond, "Cuff-less methods for blood pressure telemonitoring," *Frontiers in Cardiovascular Medicine*, vol. 6, p. 40, 2019.

[18] G. Wang, M. Atef, and Y. Lian, "Towards a continuous non-invasive cuffless blood pressure monitoring system using ppg: Systems and circuits review," *IEEE Circuits and Systems Magazine*, vol. 18, no. 3, pp. 6–26, Aug. 2018.

[19] M. Hosanee, G. Chan, K. Welykholowa, R. Cooper, P. A. Kyriacou, D. Zheng, J. Allen, D. Abbott, C. Menon, N. H. Lovell, N. Howard, W.-S. Chan, K. Lim, R. Fletcher, R. Ward, and M. Elgendi, "Cuffless

single-site photoplethysmography for blood pressure monitoring," *Journal of Clinical Medicine*, vol. 9, no. 3, 2020.

[20] A. Goldberger, Z. Goldberger, and A. Shvilkin, *Clinical Electrocardiography: A Simplified Approach E-Book*. Elsevier Health Sciences, 2017.

[21] F. S. Cattivelli and H. Garudadri, "Noninvasive cuffless estimation of blood pressure from pulse arrival time and heart rate with adaptive calibration," *2009 Sixth International Workshop on Wearable and Implantable Body Sensor Networks*, pp. 114–119, 2009.

[22] R. Shriram, A. Wakankar, N. Daimiwal, and D. Ramdasi, "Continuous cuffless blood pressure monitoring based on ptt," *2010 International Conference on Bioinformatics and Biomedical Technology*, pp. 51–55, 2010.

[23] S. Ghosh, A. Banerjee, N. Ray, P. W. Wood, P. Boulanger, and R. Padwal, "Continuous blood pressure prediction from pulse transit time using ecg and ppg signals," *2016 IEEE Healthcare Innovation Point-Of-Care Technologies Conference (HI-POCT)*, pp. 188–191, 2016.

[24] T. Le, I. Clark, J. Fortunato, M. Sharma, X. Xu, T. K. Hsiai, and H. Cao, "Electrocardiogram: Acquisition and analysis for biological investigations and health monitoring," in *Interfacing Bioelectronics and Biomedical Sensing*, Springer, 2020, pp. 117–142.

[25] M. W. Gifari, H. Zakaria, and R. Mengko, "Design of ecg homecare:12-lead ecg acquisition using single channel ecg device developed on ad8232 analog front end," in *2015 International Conference on Electrical Engineering and Informatics (ICEEI)*, 2015, pp. 371–376.

[26] D. Pani, A. Dessì, J. F. Saenz-Cogollo, G. Barabino, B. Fraboni, and A. Bonfiglio, "Fully textile, pedot:pss based electrodes for wearable ecg monitoring systems," *IEEE Transactions on Biomedical Engineering*, vol. 63, no. 3, pp. 540–549, 2016.

[27] M. Kachuee, M. M. Kiani, H. Mohammadzade, and M. Shabany, "Cuffless blood pressure estimation algorithms for continuous health-care monitoring," *IEEE Transactions on Biomedical Engineering*, vol. 64, no. 4, pp. 859–869, Apr. 2017.

[28] Q. Zhang, D. Zhou, and X. Zeng, "Highly wearable cuff-less blood pressure and heart rate monitoring with single-arm electrocardiogram and photoplethysmogram signals," *BioMedical Engineering OnLine*, vol. 16, no. 1, Feb. 2017.

[29] E. Pinheiro, O. Postolache, and P. Girão, "Theory and developments in an unobtrusive cardiovascular system representation: Ballistocardiography," *The open biomedical engineering journal*, vol. 4, pp. 201–216, 2010.

[30] C.-S. Kim, S. L. Ober, M. S. McMurtry, B. A. Finegan, O. T. Inan, R. Mukkamala, and J.-O. Hahn, "Ballistocardiogram: Mechanism and potential for unobtrusive cardiovascular health monitoring," *Scientific Reports*, vol. 6, no. 1, p. 31 297, 2016.

[31] D. D. He, E. S. Winokur, and C. G. Sodini, "An ear-worn vital signs monitor," *IEEE Transactions on Biomedical Engineering*, vol. 62, no. 11, pp. 2547–2552, 2015.

[32] P. Yousefian, S. Shin, A. Mousavi, C.-S. Kim, R. Mukkamala, D.-G. Jang, B.-H. Ko, J. Lee, U. K. Kwon, Y. H. Kim, and J.-O. Hahn, "The potential of wearable limb ballistocardiogram in blood pressure monitoring via pulse transit time," *Scientific Reports*, vol. 9, no. 1, p. 10 666, 2019.

[33] K. J. Lee, J. Roh, D. Cho, J. Hyeong, and S. Kim, "A chair-based unconstrained/nonintrusive cuffless blood pressure monitoring system using a two-channel ballistocardiogram," *Sensors (Basel, Switzerland)*, vol. 19, no. 3, p. 595, 2019.

[34] T. Hall, D. Y. C. Lie, T. Q. Nguyen, J. C. Mayeda, P. E. Lie, J. Lopez, and R. E. Banister, "Non-contact sensor for long-term continuous vital signs monitoring: A review on intelligent phased-array doppler sensor design," *Sensors (Basel)*, vol. 17, no. 11, 2017.

[35] O. T. Inan, P. Migeotte, K. Park, M. Etemadi, K. Tavakolian, R. Casanella, J. Zanetti, J. Tank, I. Funtova, G. K. Prisk, and M. D. Rienzo, "Ballistocardiography and seismocardiography: A review of recent advances," *IEEE Journal of Biomedical and Health Informatics*, vol. 19, no. 4, pp. 1414–1427, 2015.

[36] M. Jafari Tadi, E. Lehtonen, A. Saraste, J. Tuominen, J. Koskinen, M. Teräs, J. Airaksinen, M. Pänkäälä, and T. Koivisto, "Gyrocardiography: A new non-invasive monitoring method for the assessment of cardiac mechanics and the estimation of hemodynamic variables," *Sci Rep*, vol. 7, no. 1, p. 6823, 2017.

[37] I. Sadek, J. Biswas, and B. Abdulrazak, "Ballistocardiogram signal processing: A review," *Health Information Science and Systems*, vol. 7, no. 1, p. 10, 2019.

[38] Y. Haseda, J. Bonefacino, H.-Y. Tam, S. Chino, S. Koyama, and H. Ishizawa, "Measurement of pulse wave signals and blood pressure by a plastic optical fiber fbg sensor," *Sensors*, vol. 19, no. 23, 2019.

[39] M. E. Chowdhury, A. Khandakar, K. Alzoubi, S. Mansoor, A. M. Tahir, M. B. I. Reaz, and N. Al-Emadi, "Real-time smart-digital stethoscope system for heart diseases monitoring," *Sensors*, vol. 19, no. 12, 2019.

[40] A. K. Abbas and R. Bassam, "Phonocardiography signal processing," in. 2009, vol. 4, p. 218.

[41] S. Swarup and A. N. Makaryus, "Digital stethoscope: Technology update," *Medical devices (Auckland, NZ)*, vol. 11, p. 29, 2018.

[42] O. T. Inan, P. Migeotte, K. Park, M. Etemadi, K. Tavakolian, R. Casanella, J. Zanetti, J. Tank, I. Funtova, G. K. Prisk, and M. D. Rienzo, "Ballistocardiography and seismocardiography: A review of recent

advances," *IEEE Journal of Biomedical and Health Informatics*, vol. 19, no. 4, pp. 1414–1427, 2015.

[43] A. Taebi, B. Solar, A. Bomar, R. Sandler, and H. A. Mansy, "Recent advances in seismocardiography," *Vibration*, vol. 2, pp. 64–86, 2019.

[44] T. H. Huynh, R. Jafari, and W. Chung, "Noninvasive cuffless blood pressure estimation using pulse transit time and impedance plethysmography," *IEEE Transactions on Biomedical Engineering*, vol. 66, no. 4, pp. 967–976, 2019.

[45] E. J. Wang, J. Zhu, M. Jain, T.-J. Lee, E. Saba, L. Nachman, and S. N. Patel, "Seismo: Blood pressure monitoring using built-in smartphone accelerometer and camera," in *Proceedings of the 2018 CHI Conference on Human Factors in Computing Systems*, ser. CHI '18, Montreal QC, Canada: Association for Computing Machinery, 2018, pp. 1–9.

[46] A. Bilgaiyan, R. Sugawara, F. Elsamnah, C. Shim, A. Md, and R. Hattori, "Optimizing performance of reflectance-based organic photoplethysmogram (ppg) sensor," in *Proc.SPIE*, vol. 10738.

[47] M. Elgendi, R. Fletcher, Y. Liang, N. Howard, N. H. Lovell, D. Abbott, K. Lim, and R. Ward, "The use of photoplethysmography for assessing hypertension," *npj Digital Medicine*, vol. 2, no. 1, p. 60, 2019.

[48] P. Pelegris, K. Banitsas, T. Orbach, and K. Marias, "A novel method to detect heart beat rate using a mobile phone," in *2010 Annual International Conference of the IEEE Engineering in Medicine and Biology*, pp. 5488–5491.

[49] C. G. Scully, J. Lee, J. Meyer, A. M. Gorbach, D. Granquist-Fraser, Y. Mendelson, and K. H. Chon, "Physiological parameter monitoring from optical recordings with a mobile phone," *IEEE Transactions on Biomedical Engineering*, vol. 59, no. 2, pp. 303–306, 2012.

[50] K. Banitsas, P. Pelegris, T. Orbach, D. Cavouras, K. Sidiropoulos, and S. Kostopoulos, "A simple algorithm to monitor hr for real time treatment applications," in *2009 9th International Conference on Information Technology and Applications in Biomedicine*, pp. 1–5.

[51] D. Grimaldi, Y. Kurylyak, F. Lamonaca, and A. Nastro, "Photoplethysmography detection by smartphone's videocamera," in *Proceedings of the 6th IEEE International Conference on Intelligent Data Acquisition and Advanced Computing Systems*, vol. 1, pp. 488–491.

[52] M. Ghijsen, T. B. Rice, B. Yang, S. M. White, and B. J. Tromberg, "Wearable speckle plethysmography (spg) for characterizing microvascular flow and resistance," *Biomedical optics express*, vol. 9, no. 8, pp. 3937–3952, 2018.

[53] C. E. Dunn, D. C. Monroe, C. Crouzet, J. W. Hicks, and B. Choi, "Speckleplethysmographic (spg) estimation of heart rate variability during an orthostatic challenge," *Scientific Reports*, vol. 9, no. 1, May 2019.

[54] D. Jakovels, I. Saknīte, G. Krievina, J. Zaharans, and J. Spigulis, "Mobile phone based laser speckle contrast imager for assessment of skin blood flow," vol. 9421, Oct. 2014, 94210J.

[55] L. M. Richards, S. M. S. Kazmi, J. L. Davis, K. E. Olin, and A. K. Dunn, "Low-cost laser speckle contrast imaging of blood flow using a webcam," *Biomedical Optics Express*, vol. 4, no. 10, p. 2269, Sep. 2013.

[56] J. Maddury, "Arterial pulse," *Ind J Car Dis Wom*, vol. 02, no. 04, pp. 099–110, 2017.

[57] C. Pang, J. H. Koo, A. Nguyen, J. M. Caves, M.-G. Kim, A. Chortos, K. Kim, P. J. Wang, J. B. H. Tok, and Z. Bao, "Highly skin-conformal microhairy sensor for pulse signal amplification," *Advanced Materials*, vol. 27, no. 4, pp. 634–640, 2015.

[58] J. Kim, E.-F. Chou, J. Le, S. Wong, M. Chu, and M. Khine, "Soft wearable pressure sensors for beat-to-beat blood pressure monitoring," *Advanced Healthcare Materials*, vol. 8, no. 13, p. 1 900 109, 2019.

[59] K. Meng, Y. Wu, Q. He, Z. Zhou, X. Wang, G. Zhang, W. Fan, J. Liu, and J. Yang, "Ultrasensitive fingertip-contacted pressure sensors to enable continuous measurement of epidermal pulse waves on ubiquitous object surfaces," *ACS Applied Materials and Interfaces*, vol. 11, no. 50, pp. 46 399–46 407, 2019.

[60] K. Meng, J. Chen, X. Li, Y. Wu, W. Fan, Z. Zhou, Q. He, X. Wang, X. Fan, Y. Zhang, J. Yang, and Z. L. Wang, "Flexible weaving constructed self-powered pressure sensor enabling continuous diagnosis of cardiovascular disease and measurement of cuffless blood pressure," *Advanced Functional Materials*, vol. 29, no. 5, p. 1 806 388, 2019.

[61] N. Luo, W. Dai, C. Li, Z. Zhou, L. Lu, C. C. Y. Poon, S.-C. Chen, Y. Zhang, and N. Zhao, "Flexible piezoresistive sensor patch enabling ultralow power cuffless blood pressure measurement," *Advanced Functional Materials*, vol. 26, no. 8, pp. 1178–1187, 2016.

[62] C. Dagdeviren, Y. Su, P. Joe, R. Yona, Y. Liu, Y.-S. Kim, Y. Huang, A. R. Damadoran, J. Xia, L. W. Martin, Y. Huang, and J. A. Rogers, "Conformable amplified lead zirconate titanate sensors with enhanced piezoelectric response for cutaneous pressure monitoring," *Nature Communications*, vol. 5, no. 1, p. 4496, 2014.

[63] T. K. Bera, "Bioelectrical impedance methods for noninvasive health monitoring: A review," *Journal of medical engineering*, vol. 2014, pp. 381 251–381 251, 2014.

[64] M. Qu, Y. Zhang, J. G. Webster, and W. J. Tompkins, "Motion artifact from spot and band electrodes during impedance cardiography," *IEEE Transactions*

on Biomedical Engineering, vol. BME-33, no. 11, pp. 1029–1036, 1986.

[65] A. Sherwood, M. T. Allen, J. Fahrenberg, R. M. Kelsey, W. R. Lovallo, and L. J. van Doornen, "Methodological guidelines for impedance cardiography," *Psychophysiology*, vol. 27, no. 1, pp. 1–23, 1990.

[66] T. H. Huynh, R. Jafari, and W.-Y. Chung, "An accurate bioimpedance measurement system for blood pressure monitoring," *Sensors (Basel, Switzerland)*, vol. 18, no. 7, p. 2095, 2018.

[67] D. Buxi, J. Redouté, and M. R. Yuce, "Blood pressure estimation using pulse transit time from bioimpedance and continuous wave radar," *IEEE Transactions on Biomedical Engineering*, vol. 64, no. 4, pp. 917–927, 2017.

[68] A. Singh, V. Lubecke, and O. Boric-Lubecke, "Pulse pressure monitoring through non-contact cardiac motion detection using 2.45 ghz microwave doppler radar," *2011 Annual International Conference of the IEEE Engineering in Medicine and Biology Society*, pp. 4336–4339, 2011.

[69] H. Zhao, X. Gu, H. Hong, Y. Li, X. Zhu, and C. Li, "Non-contact beat-to-beat blood pressure measurement using continuous wave doppler radar," *2018 IEEE/MTT-S International Microwave Symposium - IMS*, pp. 1413–1415, 2018.

[70] J. E. Johnson, O. Shay, C. Kim, and C. Liao, "Wearable millimeter-wave device for contactless measurement of arterial pulses," *IEEE Transactions on Biomedical Circuits and Systems*, vol. 13, no. 6, pp. 1525–1534, 2019.

[71] A. Secerbegovic, J. Bergsland, P. S. Halvorsen, N. Suljanovic, A. Mujcic, and I. Balasingham, "Blood pressure estimation using video plethysmography," *2016 IEEE 13th International Symposium on Biomedical Imaging (ISBI)*, pp. 461–464, 2016.

[72] N. Sugita, M. Yoshizawa, M. Abe, A. Tanaka, N. Homma, and T. Yambe, "Contactless technique for measuring blood-pressure variability from one region in video plethysmography," *Journal of Medical and Biological Engineering*, vol. 39, no. 1, pp. 76–85, 2019.

[73] N. Sugita, T. Noro, M. Yoshizawa, K. Ichiji, S. Yamaki, and N. Homma, "Estimation of absolute blood pressure using video images captured at different heights from the heart," *2019 41st Annual International Conference of the IEEE Engineering in Medicine and Biology Society (EMBC)*, Oct. 2019.

[74] A. Chandrasekhar, J. Joseph, and M. Sivaprakasam, "A novel magnetic plethysmograph for non-invasive evaluation of arterial compliance," in *2012 Annual International Conference of the IEEE Engineering in Medicine and Biology Society*, 2012, pp. 1169–1172.

[75] Y. Lee, C. Lee, M. Kang, S. Kang, K. Kim, K. Kim, K. Kim, and J. Lee, "Magneto-plethysmographic sensor for peripheral blood flow velocity," *IEEE Sensors Journal*, vol. 14, no. 5, pp. 1341–1342, 2014.

[76] N. P.M., J. Joseph, and M. Sivaprakasam, "A magnetic plethysmograph probe for local pulse wave velocity measurement," *IEEE Transactions on Biomedical Circuits and Systems*, vol. 11, no. 5, pp. 1065–1076, 2017.

[77] B. W. Beulen, N. Bijnens, G. G. Koutsouridis, P. J. Brands, M. C. Rutten, and F. N. van de Vosse, "Toward noninvasive blood pressure assessment in arteries by using ultrasound," *Ultrasound in Medicine & Biology*, vol. 37, no. 5, pp. 788–797, 2011.

[78] A. M. Zakrzewski and B. W. Anthony, "Noninvasive blood pressure estimation using ultrasound and simple finite element models," *IEEE Transactions on Biomedical Engineering*, vol. 65, no. 9, pp. 2011–2022, 2018.

[79] P. M. Nabeel, J. Jayaraj, K. Srinivasa, S. Mohanasankar, and M. Chenniappan, "Bi-modal arterial compliance probe for calibration-free cuffless blood pressure estimation," *IEEE Transactions on Biomedical Engineering*, vol. 65, no. 11, pp. 2392–2404, 2018.

[80] J. Seo, S. J. Pietrangelo, H.-S. Lee, and C. G. Sodini, "Carotid arterial blood pressure waveform monitoring using a portable ultrasound system," *2015 37th Annual International Conference of the IEEE Engineering in Medicine and Biology Society (EMBC)*, Nov. 2015.

[81] P. S. Addison, "Slope transit time (stt): A pulse transit time proxy requiring only a single signal fiducial point," *IEEE Transactions on Biomedical Engineering*, vol. 63, no. 11, pp. 2441–2444, 2016.

[82] F. Tabei, J. M. Gresham, B. Askarian, K. Jung, and J. W. Chong, "Cuff-less blood pressure monitoring system using smartphones," *IEEE Access*, vol. 8, pp. 11 534–11 545, 2020.

[83] N. Bui, N. Pham, J. J. Barnitz, Z. Zou, P. Nguyen, H. Truong, T. Kim, N. Farrow, A. Nguyen, J. Xiao, R. Deterding, T. Dinh, and T. Vu, "Ebp: A wearable system for frequent and comfortable blood pressure monitoring from user's ear," in *The 25th Annual International Conference on Mobile Computing and Networking*, ser. MobiCom '19, Los Cabos, Mexico: Association for Computing Machinery, 2019.

[84] J. Liu, B. P. Yan, Y.-T. Zhang, X.-R. Ding, P. Su, and N. Zhao, "Multi-wavelength photoplethysmography enabling continuous blood pressure measurement with compact wearable electronics," *IEEE transactions on bio-medical engineering*, vol. 66, no. 6, pp. 1514–1525, 2019.

[85] S.-H. Liu, D.-C. Cheng, and C.-H. Su, "A cuffless blood pressure measurement based on the impedance plethysmography technique," *Sensors (Basel, Switzerland)*, vol. 17, no. 5, p. 1176, 2017.

[86] C.-S. Kim, A. M. Carek, R. Mukkamala, O. T. Inan, and J.-O. Hahn, "Ballistocardiogram as proximal timing reference for pulse transit time measurement: Potential for cuffless blood pressure monitoring," *IEEE transactions on bio-medical engineering*, vol. 62, no. 11, pp. 2657–2664, 2015.

[87] C. Kim, A. M. Carek, O. T. Inan, R. Mukkamala, and J. Hahn, "Ballistocardiogram-based approach to cuffless blood pressure monitoring: Proof of concept and potential challenges," *IEEE Transactions on Biomedical Engineering*, vol. 65, no. 11, pp. 2384–2391, 2018.

[88] S. N. Shukla, K. Kakwani, A. Patra, B. K. Lahkar, V. K. Gupta, A. Jayakrishna, P. Vashisht, and I. Sreekanth, "Noninvasive cuffless blood pressure measurement by vascular transit time," in *2015 28th International Conference on VLSI Design*, pp. 535–540.

[89] C. Hsiao, J. Horng, R. Lee, and R. Lin, "Design and implementation of auscultation blood pressure measurement using vascular transit time and physiological parameters," in *2017 IEEE International Conference on Systems, Man, and Cybernetics (SMC)*, pp. 2996–3001.

[90] A. Esmaili, M. Kachuee, and M. Shabany, "Nonlinear cuffless blood pressure estimation of healthy subjects using pulse transit time and arrival time," *IEEE Transactions on Instrumentation and Measurement*, vol. 66, no. 12, pp. 3299–3308, 2017.

[91] O. Tahar and F. Reguig, "A new approach for blood pressure estimation based on phonocardiogram," *Biomedical engineering letters*, vol. 9, pp. 395–406, 2019.

[92] A. M. Carek, J. Conant, A. Joshi, H. Kang, and O. T. Inan, "Seismowatch: Wearable cuffless blood pressure monitoring using pulse transit time," *Proc. ACM Interact. Mob. Wearable Ubiquitous Technol.*, vol. 1, no. 3, Article 40, 2017.

[93] T. Ha, J. Tran, S. Liu, H. Jang, H. Jeong, R. Mitbander, H. Huh, Y. Qiu, J. Duong, R. L. Wang, P. Wang, A. Tandon, J. Sirohi, and N. Lu, "A chest-laminated ultrathin and stretchable e-tattoo for the measurement of electrocardiogram, seismocardiogram, and cardiac time intervals," *Advanced Science*, vol. 6, no. 14, p. 1 900 290, 2019.

[94] M. Nitzan, B. Khanokh, and Y. Slovik, "The difference in pulse transit time to the toe and finger measured by photoplethysmography," *Physiological Measurement*, vol. 23, no. 1, pp. 85–93, Dec. 2001.

[95] C. Yang and N. Tavassolian, "Pulse transit time measurement using seismocardiogram, photoplethysmogram, and acoustic recordings: Evaluation and comparison," *IEEE Journal of Biomedical and Health Informatics*, vol. 22, no. 3, pp. 733–740, 2018.

[96] D. Griggs, M. Sharma, A. Naghibi, C. Wallin, V. Ho, K. Barbosa, T. Ghirmai, H. Cao, and S. K. Krishnan, "Design and development of continuous cuff-less blood pressure monitoring devices," in *2016 IEEE SENSORS*, IEEE, 2016, pp. 1–3.

[97] A. L. Goldberger, L. A. Amaral, L. Glass, J. M. Hausdorff, P. C. Ivanov, R. G. Mark, J. E. Mietus, G. B. Moody, C.-K. Peng, and H. E. Stanley, "Physiobank, physiotoolkit, and physionet: Components of a new research resource for complex physiologic signals," *circulation*, vol. 101, no. 23, e215–e220, 2000.

[98] M. Saeed, M. Villarroel, A. T. Reisner, G. Clifford, L.-W. Lehman, G. Moody, T. Heldt, T. H. Kyaw, B. Moody, and R. G. Mark, "Multiparameter intelligent monitoring in intensive care ii: A public-access intensive care unit database," eng, *Critical care medicine*, vol. 39, no. 5, pp. 952–960, May 2011, PMC3124312[pmcid].

[99] A. E. Johnson, T. J. Pollard, L. Shen, H. L. Li-Wei, M. Feng, M. Ghassemi, B. Moody, P. Szolovits, L. A. Celi, and R. G. Mark, "Mimic-iii, a freely accessible critical care database," *Scientific data*, vol. 3, no. 1, pp. 1–9, 2016.

[100] F. S. Cattivelli and H. Garudadri, "Noninvasive cuffless estimation of blood pressure from pulse arrival time and heart rate with adaptive calibration," in *2009 Sixth International Workshop on Wearable and Implantable Body Sensor Networks*, 2009, pp. 114–119.

[101] Y. Choi, Q. Zhang, and S. Ko, "Noninvasive cuffless blood pressure estimation using pulse transit time and hilbert–huang transform," *Computers & Electrical Engineering*, vol. 39, no. 1, pp. 103–111, 2013, Special issue on Recent Advanced Technologies and Theories for Grid and Cloud Computing and Bioengineering.

[102] M. Kachuee, M. M. Kiani, H. Mohammadzade, and M. Shabany, "Cuffless blood pressure estimation algorithms for continuous health-care monitoring," *IEEE Transactions on Biomedical Engineering*, vol. 64, no. 4, pp. 859–869, 2017.

[103] Y. Liang, D. Abbott, N. Howard, K. Lim, R. Ward, and M. Elgendi, "How effective is pulse arrival time for evaluating blood pressure? challenges and recommendations from a study using the mimic database," *Journal of Clinical Medicine*, vol. 8, no. 3, 2019.

[104] Y. Liang, Z. Chen, G. Liu, and M. Elgendi, "A new, short-recorded photoplethysmogram dataset for blood pressure monitoring in china," *Scientific Data*, vol. 5, no. 1, p. 180 020, Feb. 2018.

[105] R. Banerjee, A. Sinha, A. D. Choudhury, and A. Visvanathan, "Photoecg: Photoplethysmographyto estimate ecg parameters," in *2014 IEEE International Conference on Acoustics, Speech and Signal Processing (ICASSP)*, IEEE, 2014, pp. 4404–4408.

[106] Q. Zhu, X. Tian, C.-W. Wong, and M. Wu, "Ecg reconstruction via ppg: A pilot study," in *2019 IEEE EMBS International Conference on Biomedical & Health Informatics (BHI)*, IEEE, 2019, pp. 1–4.

[107] Y. LeCun, Y. Bengio, and G. Hinton, "Deep learning," *nature*, vol. 521, no. 7553, pp. 436–444, 2015.

[108] C. Wang, F. Yang, X. Yuan, Y. Zhang, K. Chang, and Z. Li, "An end-to-end neural network model for blood pressure estimation using ppg signal," in *Artificial Intelligence in China*, Springer, 2020, pp. 262–272.

[109] G. Slapničar, N. Mlakar, and M. Luštrek, "Blood pressure estimation from photoplethysmogram using a spectro-temporal deep neural network," *Sensors*, vol. 19, no. 15, p. 3420, 2019.

[110] J. Lee, S. Sun, S. M. Yang, J. J. Sohn, J. Park, S. Lee, and H. C. Kim, "Bidirectional recurrent autoencoder for photoplethysmogram denoising," *IEEE journal of biomedical and health informatics*, vol. 23, no. 6, pp. 2375–2385, 2018.

[111] H.-T. Chiang, Y.-Y. Hsieh, S.-W. Fu, K.-H. Hung, Y. Tsao, and S.-Y. Chien, "Noise reduction in ecg signals using fully convolutional denoising autoencoders," *IEEE Access*, vol. 7, pp. 60 806–60 813, 2019.

[112] G. Montavon, W. Samek, and K.-R. Müller, "Methods for interpreting and understanding deep neural networks," *Digital Signal Processing*, vol. 73, pp. 1–15, 2018.

[113] N. Xie, G. Ras, M. van Gerven, and D. Doran, "Explainable deep learning: A field guide for the uninitiated," *arXiv preprint arXiv:2004.14545*, 2020.

[114] H. Jeong, J. A. Rogers, and S. Xu, *Continuous on-body sensing for the covid-19 pandemic: Gaps and opportunities*, 2020.

[115] A. L. Mueller, M. S. McNamara, and D. A. Sinclair, "Why does covid-19 disproportionately affect older people?" *Aging*, vol. 12, no. 10, 2020.

[116] J. Kim, E.-F. Chou, J. Le, S. Wong, M. Chu, and M. Khine, "Soft wearable pressure sensors for beat-to-beat blood pressure monitoring," *Advanced healthcare materials*, vol. 8, no. 13, p. 1 900 109, 2019.

[117] K.-H. Huang, F. Tan, T.-D. Wang, and Y.-J. Yang, "A highly sensitive pressure-sensing array for blood pressure estimation assisted by machine-learning techniques," *Sensors*, vol. 19, no. 4, p. 848, Feb. 19, 2019.

[118] K. Kario, Y. Morisawa, A. Sukonthasarn, Y. Turana, Y.-C. Chia, S. Park, T.-D. Wang, C.-H. Chen, J. C. Tay, Y. Li, *et al.*, "Covid-19 and hypertension—evidence and practical management: Guidance from the hope asia network," *The Journal of Clinical Hypertension*, vol. 22, no. 7, pp. 1109–1119, 2020.

[119] M. Vaduganathan, O. Vardeny, T. Michel, J. J. McMurray, M. A. Pfeffer, and S. D. Solomon, "Renin–angiotensin–aldosterone system inhibitors in patients with covid-19," *New England Journal of Medicine*, vol. 382, no. 17, pp. 1653–1659, 2020.

TAI LE (S'17) received the Engineering degree in Electronics and Telecommunications from Hanoi University of Science and Technology, Hanoi,Vietnam, in 2016. He was a research student with the University of Washington, Bothell campus, in 2017. He is currently pursuing the Ph.D. degree with the University of California at Irvine, Irvine, CA, USA. His research includes bio-signal processing, bio-instrumentation, and bio-sensors.

FLORANNE ELLINGTON was born in San Francisco, California. She received her B.S. degree in Computer Engineering from the University of California, Irvine. In 2019, she joined the Department of Electrical Engineering and Computer Science at the University of California, Irvine as a Ph.D. student to earn her M.S. and Ph.D. degrees in Computer Engineering. Her research interests include embedded systems and machine learning analysis applications to healthcare devices.

TAO-YI LEE (S'11) was born in Taichung, Taiwan. He received B.S. and M.S degrees in Electronics Engineering from National Chiao-Tung University, Taiwan. He also received M.S. degree in Computer Science from University of California, Irvine. In 2018, he joined the Department of Computer Science at University of California, Irvine, as a Ph.D. student. His research interests include embedded systems, healthcare machine learning algorithms, and low-power electronics.

KHUONG VO received his B.Eng. degree in Computer Science from Vietnam National University, Ho Chi Minh City, in 2017. In 2019, he joined the Department of Computer Science at the University of California, Irvine, to pursue a Ph.D. degree. His research interests include biomedical signal processing and internet of things in healthcare.

MICHELLE KHINE, PH.D. is a Professor of Biomedical Engineering at UC Irvine. She is the founding Director of Faculty Innovation at the Samueli School of Engineering and founding Director of BioENGINE (BioEngineering Innovation and Entrepreneurship) at UC Irvine. Prior to joining UC Irvine, she was an Assistant and Founding Professor at UC Merced. Michelle received her BS and MS from UC Berkeley in Mechanical Engineering and her PhD in Bioengineering from UC Berkeley and UCSF. She develops point of care technologies and stretchable electronics for democratized, decentralized healthcare. She is the Scientific Founder of 6 start-up companies. Michelle was the recipient of the TR35 Award and named one of Forbes '10 Revolutionaries' in 2009 and by Fast Company Magazine as one of the '100 Most Creative People in Business' in 2011. She was awarded the NIH New Innovator's Award, was named a finalist in the World Technology Awards for Materials, and was named by Marie-Claire magazine as 'Women on Top: Top Scientist'. She was named Innovator of the Year 2017 for the Samueli School of Engineering at UC Irvine. Michelle is a Fellow of AIMBE (American Institute of Medical and Biological Engineering) and well as a Fellow of the National Academy of Inventors.

SANDEEP KRISHNAN, MD, FACC, FSCAI completed his fellowship in interventional cardiology and structural/valvular heart disease at the University of Washington School of Medicine in Seattle, WA. He graduated summa cum laude from the University of Missouri-Kansas City School of Medicine and graduated with distinction from internal medicine residency at Emory University School of Medicine. He completed a cardiovascular diseases fellowship at the Cedars-Sinai Heart Institute where he was selected for the coveted and highly prestigious ACC/Merck fellowship awarded to only four cardiology fellows across the country for fellow-initiated research in 2016. The fellowship provides grant money of $70,000 to support a fellow-initiated research project. Sandeep performed cutting edge work examining the relationship of vulnerable coronary plaque features to cardiac computed tomography findings. Dr. Krishnan has held several leadership positions in medical education at all levels including serving on the ACGME Board of Directors as a resident member in 2016-2018 and serving on the National Resident Matching Program Board of Directors as a medical student member from 2007 to 2009. Additionally, Krishnan serves in various leadership positions within the American College of Cardiology including serving on the Health Affairs Committee, the Board of Trustees Medical Malpractice Working Group, and the PAC Advisory Council. He has been recognized as a future leader of the college and was part of the ACC's Leadership Academy and Emerging Advocates cohorts. Sandeep has also remained active in the AMA throughout his career and was most recently chairman of the Committee of Business and Economics in 2015-2016. He currently serves as the Director for Structural Heart Disease and the Director of Heart Failure Programs at King's Daughters Medical Center in Ashland, KY. When he is not busy with teaching internal medicine and family practice residents in his practice as an interventional and structural cardiologist, Sandeep enjoys rock climbing, playing the piano, and swimming. He is a voracious reader and accomplished technical writer as well.

NIKIL DUTT (F) is a Distinguished Professor of CS, Cognitive Sciences, and EECS at the University of California, Irvine, and also a Distinguished Visiting Professor of CSE at IIT Bombay, India. He received a PhD from the University of Illinois at Urbana-Champaign (1989). His research interests are in embedded systems, EDA, computer architecture and compilers, distributed systems, healthcare IoT, and brain-inspired architectures and computing. He has received numerous best paper awards and is coauthor of 7 books. Professor Dutt has served as EiC of ACM TODAES and AE for ACM TECS and IEEE TVLSI. He is on the steering, organizing, and program committees of several premier EDA and Embedded System Design conferences and workshops, and has also been on the advisory boards of ACM SIGBED, ACM SIGDA, ACM TECS and IEEE ESL. He is an ACM Fellow, IEEE Fellow, and recipient of the IFIP Silver Core Award.

HUNG CAO (S'06–M'12–SM'15) received his B.Sc. degree in Electronics and Telecommunications from Hanoi University of Science and Technology, Vietnam in 2003. He then served as a lecturer at Vietnam Maritime University from 2003 to 2005. He got his M.Sc. and Ph.D. in Electrical Engineering from the University of Texas at Arlington in 2007 and 2012, respectively. After his Ph.D. study on biosensors and bioelectronics, Dr. Cao received training in bioengineering and medicine at University of Southern California (2012-2013) and University of California, Los Angeles (2013-2014). In 2014-2015, he worked for ETS, Montreal, QC, Canada as a research faculty. From Fall 2015 to Summer 2018, Dr. Cao worked as an Assistant Professor of Electrical and Biomedical Engineering at University of Washington, Bothell campus. Dr. Cao joined the Department of Electrical Engineering and Computer Science, UC Irvine from September 2018. Dr. Cao is a recipient of the prestigious National Science Foundation (NSF) CAREER Award (2017). His research has been funded by his home institutions, NSF, National Institute of Health (NIH) and industry partners.